ADDIS ABABA UNIVERSITY
SCHOOL OF GRADUATE STUDIES

# ELECTROCHEMICAL SYNTHESIS AND CHARACTERIZATION OF POLYMERS AND COPOLYMERS OF 3-HEXYLTHIOPHENE, 3-METHYLTHIOPHENE AND 3-OCTYLTHIOPHENE

GETACHEW ADAM

JUNE 2005
ADDIS ABABA

# DECLARATION

I, the undersigned, declare that this thesis is my original work and has not been presented for a degree in any other University and that all the sources of materials used for this thesis has been duly acknowledged.

Name: Getachew Adam

Signature: _____

This thesis has been submitted for examination with my approval as University Advisor.

Name: Dr. Teketel Yohannes

Signature:_____

Place and Date of Submission: Department of Chemistry

Addis Ababa University

June 2005

## TABLE OF CONTENTS

**Page**

## LIST OF FIGURES

**Figure** **Page**

# ABSTRACT

The electrochemical polymerizations and characterization studies were made for the monomers 3-hexylthiophene (3HT), 3-methylthiophene (3MT) and 3-octylthiophene (3OT).The electrochemical properties of the corresponding polymers poly(3-hexylthiophene) (P3HT) , poly(3-methylthiophene) (P3MT) and poly(3-octylthiophene) (P3OT) were also studied in a monomer free $LiClO_4$ - acetonitrile solutions. Copolymers were electrochemically synthesized from the monomers and showed intermediate electrochemical properties between their corresponding homopolymers. The first copolymer obtained was the copolymer of 3HT and 3OT (poly(3HT-co-3OT)) from 1:1.5 volume ratio of 3HT to 3OT at a potential of 1.70 V in 0.1 M $LiClO_4$ - acetonitrile solution and the second was the copolymer of 3MT and 3OT, (poly(3MT-co-3OT)) from 1:2.5 volume ratio of 3HT to 3OT at a potential of 2.00 V in $LiClO_4$ - acetonitrile solution.

The electrocatalytic effects of the polymers and copolymers electrochemically modified on platinum disc electrode were examined using ferricyanide redox system. Among the polymers examined a copolymer of 3MT and 3OT showed the best electrocatalytic effect. Based on this result the electrocatalytic effect of this copolymer was further studied on selected environmental and biological samples. It was found that poly(3MT-co-3OT) modified platinum electrode is highly selective and sensitive towards

a) detection of ferricyanide with the detection limit of 20 μM, in 1 M aqueous potassium nitrate solution using cyclic voltammetry,
b) simultaneous detection of the isomeric compounds hydroquinone and catechol with a detection limit of 40 μM for both analytes in phosphoric acid solution pH = 0.5 using differential pulse voltammetry,
c) detection of ascorbic acid with a detection limit of 80 μM in phosphate buffer solution pH = 4.0 using differential pulse voltammetry,
d) selective detection of catechol in the presence of the known interferance asorbic acid with a detection limit of 80 μM in phosphate buffer solution pH = 4.0 using differential pulse voltammetry.



***Key words***; *poly(3-hexylthiophene), poly(3-methylthiophene), poly(3-octylthiophene), poly(3HT-co-3OT), poly(3MT-co-3OT), Electrochemical Polymerization*, *Electrocatalysis*.

## 1. INTRODUCTION

The scientific impulse is to create better materials with ecologically demanding, enviromental friendly and improved properties. The materials that are used in an electrochemical devices are mostly metals and inorganic semiconductros which are expensive, scarce and highly susceptible to corrosion. Therefore the future needs sustainable, stable, cheap and easily accessable materials for electrochemical devices.

Conjugated polymers having semiconductor and conductor properties become the most promising materials to be used in electrochromic devices [1], as catalysts [2a], as sensors [2b], as electrochemomechanical devices [3], as modified electrodes [4], as photovoltic devices [5], and in a corrosion protection [6], etc. Most of the known conducting polymers today were first synthesized chemically as insulating powder or film. The interest in organic conducting polymer increased when one was able to synthesize a polymer in its conductive state (doped form) using electrochemical technique. Furthermore, the possibility of modifying the polymers through side chains and copolymerization has opened up new options for use as active components in photoelectrochemical [7-9] and electrochemical devices [10-13].

Modification of the form, structure, and properties of a conducting polymer is mandatory to meet the specific requirements for different technological applications. The selection of the proper method of modification depends on both the desired property and the level at which the modification will occur. Copolymerization is one method of modification, and results in copolymers with properties intermediate between the individual polymers. Many types of copolymers have been prepared by chemical and electrochemical polymerization from mixtures of different monomers [14-20]. From the polymers or copolymers obtained from the appropriate modification a better performance could be achieved when compared to the corresponding unmodified or parent polymers.

These polymers and copolymers are now competing with the classical surfaces such as metals and carbon in electrochemical applications. Some aspects making modified electrodes look attractive as electrochemical tools are the possibility of preconcentrating the analyte near or at the electrode surface, the high selective nature of the modified surface and its remarkable

sensitivity. The implementation of the above properties of polymers along with some specific catalytic activity will result in minimizing high background currents by the suppression of competing redox reactions. Fouling of the electrode surface has long been a serious problem in electrochemical determinations of many organic compounds. Polymer coating of the surface of the electrode substrate helped to alleviate this problem [21].

In this study polymers and copolymers of 3-hexylthiophene, 3-octylthiophene and 3-methylthiophene were electrochemically synthesized and characterized using various techniques for their use as electrochemical active devices such as batteries, electrochromic devices, micromuscles, photoelectrochemical cells, and electrocatalysis. In particular electrocatalysis at conducting polymer electrodes using the aforementioned polymers and copolymers was studied on environmental and biological samples such as potassium ferricyanide, ascorbic acid, catechol and hydroquinone. Among which the copolymer of 3-methylthiophene and 3-octylthiophene (poly(3MT-co-3OT)) showed a promising result for the electrocatalytic detection of the above analytes (redox species) in terms of selectivity as well as sensitivity when a platinum electrode was modified with this polymer.

## 2. LITERATURE REVIEW

### 2.1 The Structure of Conjugated Polymers

Carbon has the electronic configuration $1s^2 2s^2 2p^2$ and forms four nearest neighbor bonds. In σ-bonded polymers, as in polyethylene (PE) which consists of the monomeric repeated unit of -($CH_2$-$CH_2$)-, the C atoms are $sp^3$ hybridized, and each C atom has four σ-bonds. In such non conjugated polymers, the electronic structure of the chain of atoms that comprises the backbone of the macromolecule consists of only σ-bonds. The large energy band gaps in σ-bonded polymers, $E_g$ ( σ ), renders these polymer materials electrically insulating, and generally non absorbing to visible light. In polyethylene, for example, the optical band gap is of the order of 8 eV [22].

In conjugated polymers, however, there exists a continuous network, often a simple chain, of adjacent unsaturated carbon atoms, i.e., carbon atoms with $sp^2$ hybridized state. Each of these $sp^2$ hybridized C atoms has three σ-bonds, and the remaining $p_z$ atomic orbital, which exhibits

π-overlap with the $p_z$ orbital of the nearest neighbor $sp^2$ hybridized C atoms. This chain of atoms with π-overlap of the atomic $p_z$-orbitals leads to the formation of π-states delocalized along the polymer chain. In a system with one dimensional periodicity, these π-states form the electronic bands, accounting for optical absorption at lower photon energies.

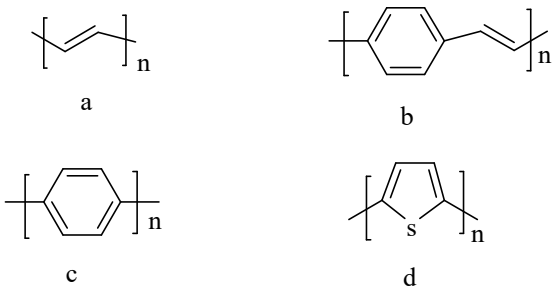


Figure 1. The structural formula of some common polymer chains.
(a) *trans*-polyacetylene, (b) poly(*para*-phenylenevinylene),
(c) poly(*para*-phenylene), (d) poly(thiophene)

The essential properties of the delocalized π-electron system, which differentiate a typical conjugated polymer from a conventional polymer with σ-bonds, are the following;

(i) The electronic band gap, $E_g$ is relatively small (~1- 4 eV), leading to low energy electronic excitations and semiconductor behavior,

(ii) The polymer chains can easily be oxidized or reduced, through charge transfer with dopant species,

(iii) Carrier mobilities are large and high electrical conductivities are realized in the doped (chemically/electrochemically oxidized or reduced) state, and

(iv) The mobile charge carriers are not free electrons or holes, but quasi-particles, which may move freely through the material, along uninterrupted polymer chains.

Conjugated polymers are quasi one dimensional, with a covalent bonding within the chains and interactions between chains are of Van der Waals type. The intrinsic geometrical structure is dependent upon the ionic state of the polymer, which leads to the existence of the unusual charge carrying species. The charge bearing species are not free electrons or holes, but may be any one of several different types of quasi particles, each consisting of a coupled charge lattice deformation entity. The charge bearing species are self localized, and the presence of

electronic charge leads to local changes in the geometry (the lattice), which in turn, leads to localized changes in the electronic structure. These species can be generated through optical absorption, or through charge transfer, which later on becomes localized electronic states with energy levels within the forbidden electron energy gap.

Note that in *trans*-polyacetylene (Fig.1a), an interchange of the carbon-carbon single (-) and double (=) bonds reproduces the identical ground state geometry. Thus, *trans*-polyacetylene is termed as a degenerate ground state system. This geometric symmetry has consequences for the nature of the self-localized charge bearing species, which are termed as *solitons*. In the remaining conjugated polymers (Fig.1b, c, and d), a simple interchange of the carbon-carbon single and double bonds does not reproduce the same ground state geometric configuration, but produces higher energy geometric configurations [23]. Thus, these polymers are termed as non degenerate ground state systems. This symmetry also has consequences for the type of charge bearing species.

Excess electrons added to any conjugated polymer chain lead to new electronic states within the forbidden electron energy gap, as shown for a non degenerate ground state system in Figure 2. In principle, the first electrons added to any conjugated polymer chain form singly charged polarons. In chemical terminology, a polaron is a radical ion in association with a local geometry relaxation. In the case of *trans*-polyacetylene, it has been established that pairing up of polarons leads to spinless, singly charged solitons that represent the lowest energy eigen states of the coupled electron (hole) lattice systems, and are responsible for the unusual electrical, magnetic and optical properties.

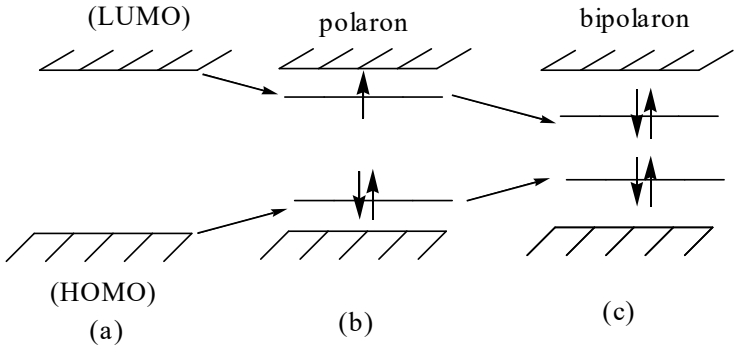


Figure 2. Energy level scheme of the self localized states in conjugated polymers:
(a) band edges of a neutral polymer (b) polaron (c) spinless bipolaron.

On the other hand, in non-degenerate ground state conjugated polymers, the polarons can pair up to form spinless, doubly charged bipolarons [24].

### 2.2 Doping and Undoping

Since a conjugated polymer is a semiconductor with a finite band gap, conversion into a conductor requires an introduction of charges in to the polymer chain, using various methods. The first method is the introduction of charges either by electron removal with oxidants like $I_2$, $FeCl_3$, (p-doping) or injection of electron by reducing agents like Na (n-doping) [25].

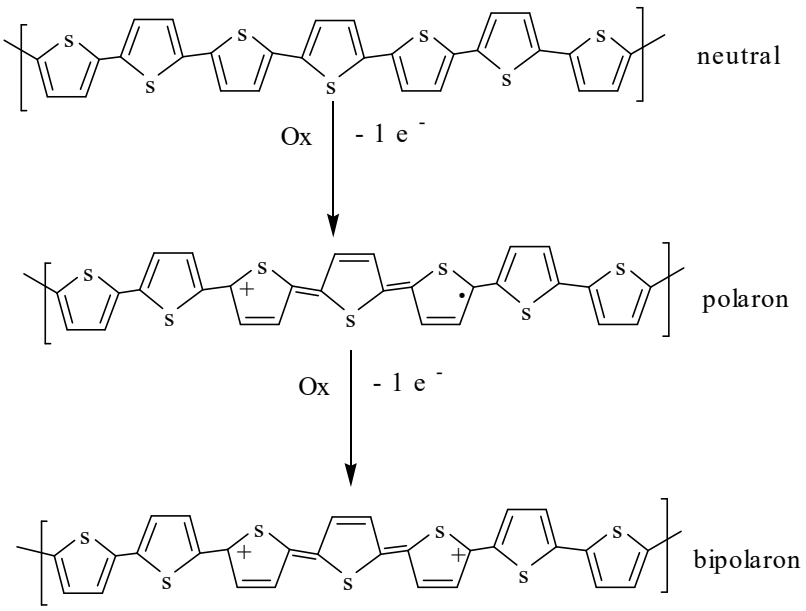


Scheme 1. Structural changes in polythiophene upon doping with a suitable oxidant.

Most of the conjugated polymers known today are p-type semiconductors, which can be doped with oxidants. The structural changes that occur in a conjugated polymer upon oxidation are illustrated in Scheme 1 for polythiophene [26]. The removal of one electron from the polythiophene chain produces a mobile charge in the form of a radical cation, also called a polaron. Further oxidation can either convert the polaron into a spinless bipolaron or introduce another polaron. A bipolaron is thus a di-ion around which a strong, localized lattice relaxation occurs. In either case, introduction of each positive charge also means introduction of a negatively charged counter ion.

In the doped state the conjugated polymers possess a very high electronic conductivity, up to 100 or even 1000 S/cm. The conventional theory attributes it to a high mobility of single charged polarons whose theoretical calculations of the electronic structure of the polymer molecule lead to the conclusion that there is a gain in energy if two polarons form a bipolaron [27].

In the same way doping of poly(3-alkylthiophenes) (P3ATs) is achieved by either chemical oxidation with oxidants such as $I_2$ or $FeCl_3$, or by electrochemical oxidation of thin polymer films in the presence of an electrolyte such as tetraethylammonium tetrafluoroborate (TEATFB) or lithiumperchlorate ($LiClO_4$). Apart from the drastic increase in electrical conductivity, other more important property changes have also been observed on doping. Doping greatly affects the flexibility of polymer chains. The barrier to rotation of the repeating units along the polythiophene chain has been found to increase by 10 to 100 times when doped. This results in an increase in stiffness, which renders the doped segments more planar and extended than the undoped portions. This can be translated into an increase in volume on doping. Based on this idea a class of conjugated materials prepared by cross-linking P3ATs or copolymers of P3ATs have been produced and investigated [28].

One of the major problems with conducting P3ATs is their thermal unstability that is closely related to the ease of undoping. At $100^0$C, the conductivity of P3AT thin films is markedly decreased within minutes [29]. The rate of thermal undoping is controlled by the steric interaction between alkyl chains and dopants, which increases with enhanced movements of the side chains at high temperatures. One way to prepare materials, which are more thermally stable in terms of undoping, is to decrease the interaction between the side chains and dopants. A random copolymer was produced from 3-octylthiophene and 3-methylthiophene, which showed a higher thermal stability [30].

### 2.3 Electrochemical Polymerization

The electrochemical polymerization is carried out with a classical three electrode electrochemical cell, consisting of a working electrode, a reference electrode and a counter electrode and an electrolyte solution containing the monomer in a supporting electrolyte

solution. A solvent is used in which the monomer is soluble but not the polymer. The nature of the working electrode is critical for the preparation of these films and depends on the type of polymer to be synthesized and on the electrolyte medium [31]. Since oxidative or reductive processes produce the films, it is important that the electrode should not oxidize or reduce concurrently with the monomer. Working electrodes such as gold, platinum and transparent indium doped tinoxide (ITO) coated glass can be used. The ITO-coated glass electrode is particularly suitable for spectroscopic studies.

Electrochemical synthesis of conjugated polymers has the following advantages over the chemical synthesis.

a) The polymeric material is produced in one step, directly grafted onto the electrode surface.
b) There is no need for a catalyst; therefore, the electrodeposited polymer is pure.
c) By controlling the amount of charge supplied, the thickness of the polymer film may be controlled from a few angstroms to many micrometers.
d) By changing the nature of the counter ions in solution, the electrical and physico-chemical properties of the polymer may be changed for a particular purpose.
e) It is possible to perform *in situ* characterization of the growth process of the polymer by electrochemical and/or spectroscopic techniques [32, 33].

For the synthesis, potentiostatic (fixed potential), galvanostatic (fixed current), or potentiodynamic (varying potential) methods can be used. A preliminary study is necessary in order to find a solvent in which the monomer is soluble and to determine the potential at which the polymerization may be performed. Cyclic voltammetry is a very good technique to determine the best polymerization conditions. The polymerization potential should not be too low, since this causes the polymerization process to be very slow and to form soluble oligomers, nor too high in order to avoid a material having lower conductivity due to overoxidation. In general, the polymerization potential must be chosen not too far (± 0.1 V) from the corresponding oxidation peak potential of the monomer.

The electrodepositing potential is specific for any given electropolymerization process. As the potential needed for monomer oxidation is always higher than the charging of the existing polymer, both polymerization and doping processes may be driven by a single electrochemical operation which, starting from the monomer, first forms the polymeric chain and then induces its oxidation/reduction and deposition on the working electrode. The electrochemical properties of the polymeric film coating the working electrode can be studied *in situ* or afterwards in monomer free solution.

The general mechanism of electrochemical polymerization of thiophene and its alkyl substituted derivatives appears to follow the Scheme 2 shown below [34]. The first step consists of the electrochemical oxidation of the neutral monomer to form delocalized radical cations. Since the electron transfer reaction is much faster than the diffusion of the monomer from the bulk solution, a high concentration of radicals is continuously maintained at the electrode/solution interface. It is followed by the combination of two radical cations to form a dimer and then loses two protons to become electrically neutral. This dimer, which is more easily oxidized than the monomer, is further oxidized to a radical cation, and react with other radical cations. Chain growth proceeds between the radical cations of the monomer and those of the continuously forming oligomers. The cation radical formation leads to a very rapid dimerization step. A significantly greater stability of the double charged dimer prevents its dissociation to the same radicals during the reduction scan. This finding has led to assume that similar physical phenomena might take place inside the polymer films where the creation of radical cations at the matrix may induce the creation of intermolecular bonds whose decomposition can only occur at a much more negative potential, thus leading to a hysteresis in cyclic voltammetry curves. In order to sustain film growth at the electrode surface the electrode potential has to be maintained at the electrical oxidation potential of the monomer. The electrochemical reaction proceeds through successive electrochemical and chemical steps (Scheme 2).

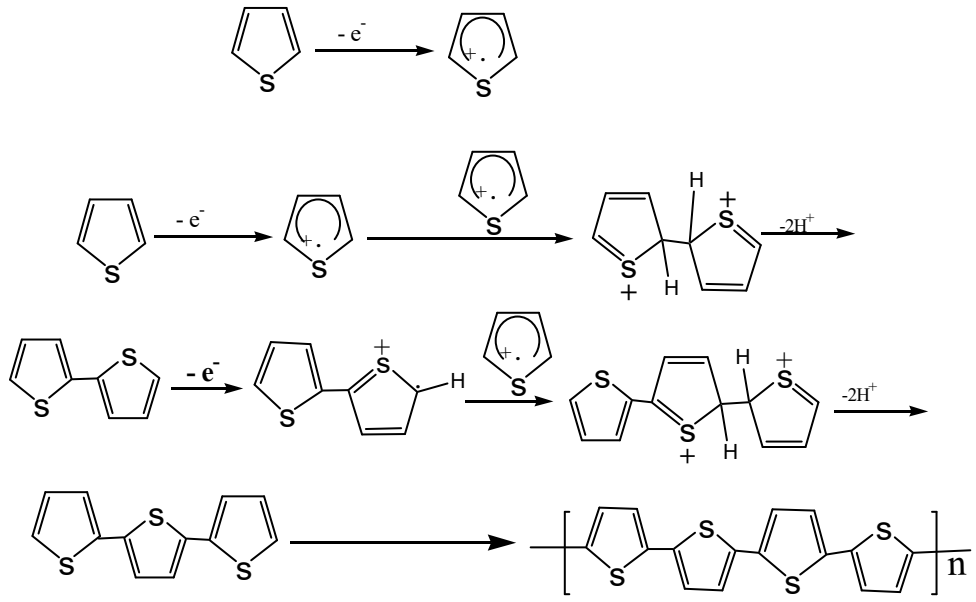

Scheme 2. Mechanism of electropolymerization of thiophene.

Polythiophene (PT) has always been one of the most likely candidates to be used in electrochemical devices because of its high stability in doped and undoped states, its ease of structural modification, and its controllable electrochemical behavior. poly(3-alkylthiophene)s (P3ATs) and other substituted thiophenes, which can be highly processed have been the subject of intense research and development in the past. Studies demonstrated that polythiophene belongs to one of the few cases in which substitution of hydrogen at the 3-position by an alkyl chain does not affect the conductivity of the polymer, while imparting solubility and consequently enhanced processability [35].

**2.4 Functionalization of conjugated backbones with electron donating groups**

For sometime the application of conducting polymers has been limited due to their intractability and insolubility, especially in the doped state. This problem was overcame by functionalization of the conjugated backbones with electron donating groups [36]. This allowed the polymers obtained to be easily processed and fully characterized by chemical, electrochemical and physical methods.

Although the substitution of electron donating groups does not lead directly to low band gap materials, it is the most straight forward approach towards reducing the band gap of a conjugated backbone. On the basis of electronic effects alone, the energy of absorption decreases with alkyl substitution and is further diminished with alkoxy functionalization. The presence of electron donating substituents raise the energy of the highest occupied molecular orbital (HOMO) with a consequent narrowing of the energy band gap (as evident from a comparison of polythiophene with 3-functionalized polythiophene [37]). These electronic effects are in contrast to increased steric effects upon functionalization with pendant groups, which are anticipated to raise the band gap by reducing coplanarity and therefore the extent of conjugation in the polymer backbone. It should be noted also that any correlation between band gap and the electronic effects of the 3-substituents are to be interpreted with caution particularly since both stereoregularity and regioregularity, have significant effects on band gap values.

**2.5 Copolymers**

Polymer chains composed of two or more different monomer units are called copolymers. Copolymer properties depend strongly on the primary structure of the monomers, i.e. on the way the various monomers distribute along the chain. If we have two different monomers A and B we can define (as extreme cases) alternate copolymers (---ABABABAB--) and block copolymers (---AAABBBAAABBB---), intermediate cases are characterized by a distribution in the lengths of A and B blocks, respectively, and of course, by the overall composition. A copolymer is called random when there is no correlation in the monomer distribution along the chain, and statistical when there is some correlation such that the sequence corresponds to a biased selection from the appropriate mixture of A and B. As a consequence, any statistical copolymer sample is essentially a mixture of many different chains [38]. Random copolymers of alkylthiophenes such as copolymers of 3-octylthiophene and 3-methylthiophene were prepared electrochemically and upon doping these copolymers were more thermally stable than the homopolymers [39].

## 2.6 Cyclic Voltammetry

One of the electrochemical techniques that is often used to study the electrochemical properties of conjugated polymers is cyclic voltammetry. It is a technique where the cell current is measured while sweeping the potential applied between the working electrode and the reference electrode. It represents the principal source of experimental information on the charging and discharging processes of conducting polymers. The charging is shown as a steep anodic wave followed by a broad flat plateau as the potential increases. It has been suggested that the plateau is related to capacitive charging of double layers of the system. In the reverse scan a potential shifted cathodic wave appears at the low potential end of the plateau with a peak height of about half the value of the anodic peak. This is different from the ideal symmetrical waves for a material adsorbed on electrode with identical cathodic and anodic peaks. This is because of the fact that there is an interaction between charged sites and there are differences between the neutral and doped state regarding conformation as well as transport properties [40].

The above concept of polarons and bipolarons was applied to the interpretation of these cyclic voltammetry data, where the hysteresis of the current was attributed to the slow transformation of the neutral sites of the polymer matrix into polarons and then polarons in to bipolarons [41]. An alternative treatment was proposed by Feldberg [42] who suggested to distinguish between the faradaic current to oxidize the polymer matrix itself and a capacitive contribution to charge the interface between the charged matrix and the ion solvent phase. As for the interpretation of cyclic voltammetric curves, the above concept attributes usually peaks to the faradaic process while the plateaus of the current to the capacitive term. The latter contribution is too great to be ascribed to the interface between the polymer phase containing the matrix as well as counter ions and solvent molecules between polymer chains and the solution in macropores. Another variant of this approach attributes the capacitive term to the charging of the interface between polymer chains and counter ions i.e. this concept considers these components as representing two phases which can hardly be justified physically. However, this explanation of cyclic voltammetry plateaus leaves without an explanation the CV data for conducting oligomers [43], which can be oxidized up to a similar charging level, but their CV curves represent a series of separate peaks without any plateaus. Moreover, a

stronger oxidation of such films leads to the chemical dimerization of those molecules, and this process is accompanied with smearing out the peaks, with a gradual appearance of the plateaus typical for conducting polymers [44].

A strong hysteresis of anodic and cathodic peaks may also be a consequence of the specific form of the relation between the energy of the system and its charging level [45] and because of electrostatic interaction between electronic and ionic charge carriers inside the film [46]. Then, the continuous charging or discharging process within certain potential intervals changes at some points to a stepwise one due to the phase transition leading to the jump of the system from the initial state, which has become unstable, to a new stable one. This approach enables one to explain why the drastic change of the electronic conductivity (insulator-to-conductor or *vice versa*) takes place within the cyclic voltammetry peaks.

Although the cyclic voltammograms of conducting polymers have different shapes depending on the type and polymerization conditions, some common features can often be observed. The position of the peaks has been shown to depend on conjugation length. With increasing conjugation length the respective oxidation and reduction potentials shift towards lower energies. Substitution also influences the position of the peaks in such a way that electron donating substituents lower the oxidation potential and the electron withdrawing groups raise the potentials. One prominent characteristic of the cyclic voltammograms of poly(3-alkylthiophene) (P3AT) is the less sharper redox peaks for the P3AT as compared to poly(dialkylbithiophene) [47]. The large half-width of the redox peaks is a general phenomenon in substituted polythiophenes obtained from nonsymmetric monomers and is associated with the presence of coupling defects which, when distributed statistically, result in a series of energetically nonequivalent chain segments.

The band gaps of conjugated polymers can be evaluated from the onset oxidation/reduction potentials in the polymer cyclic voltamograms which can be correlated to the ionization potential (IP) and electron affinity (EA) respectively, from which band gap can be determined by taking differences. So that correlation of the electrochemically derived band gap with values from the optical absorption spectra of thin films can be made [48].

A further lowering of the band gap by electron donating groups is limited by the steric effects of the substituents on adjacent thiophene rings which forces the rings out of coplanarity. The torsions introduced into the $\pi$-system of the polythiophene backbone result in the energy absorption maxima shifting to higher energies whilst the band gap, is also increased. Clear differences are evident from the electronic absorption spectra of regioregular and nonregioregular P3ATs in thin-film UV-Vis absorption maxima, where $\lambda_{max}$ (polymer $\pi$-$\pi$* transition), is clearly dependent upon the arrangement of monomer units in the polymer. Here, unfavorable steric effects from the alkyl pendant substituents on adjacent rings in the arrangement have the effect of creating a sterically driven twist from coplanarity with a consequent reduction in the effective conjugation lengths in the polymer. The studies on the optical and electrical properties of P3AT as a function of alkyl chain length and ambient conditions concluded that [37]:

(i) Both the melting point ($T_m$) and glass transition temperature ($T_g$) decrease with increasing alkyl side chain length;

(ii) conductivity decreases with increasing alkyl chain length;

(iii) The absorption peak of P3AT shifts to shorter wavelengths (higher energies) with increasing temperatures; and

(iv) The temperature at which the absorption peak shift occurs becomes lower with increasing side chain length.

The reduction of the energy band gap has been a research goal for conducting polymers so that the absorption of the undoped polymer shifts from the visible towards the near infrared region of the electromagnetic spectrum. The following outlines are some of the impetus/rationale towards the development of low band gap materials [37]:

a) A smaller band gap-conducting polymer would facilitate the ease of doping with the possibility of achieving intrinsic metallic conductivity.
b) These materials would possess improved photoconductivities.
c) They are likely to afford transparent materials in the doped state.

## 2.7 Electrocatalysis at conducting polymer electrodes

For electroanalytical purposes, electrocatalysis at chemically or electrochemically modified electrodes are used to amplify the detection signal. It accelerates the heterogeneous electron transfer of the target analyte, which is slow at the same potential at a bare electrode, induced by an immobilized charge mediator, i.e., catalyst. Electrocatalysis at a modified electrode needs to be distinguished from mediation. Mediation implies that an immobilized redox couple generates heterogeneous electron transfer of a target redox analyte in solution that would occur just as readily at the same potential at a bare electrode if it were available.

Slow electrode reactions of many important analytes require a potential greatly exceeding their formal redox potentials in order for the reactions to proceed at desirably high rates. The acceleration of such kinetically hindered electrode reactions by electrode-confined charge mediators permits the quantification of these analytes at less extreme potentials, because catalyzed electrode reactions usually occur near the formal potential of the mediator. By applying less extreme potentials, both detectability and selectivity can be improved significantly, as compared with those obtained at non-modified electrodes. Also, the electrode fouling is decreased which may occur in case of direct electrochemical conversion of the analyte at more extreme potentials at a bare electrode. Variations of the formal redox potential of the immobilized catalyst can be used effectively to discriminate between analytes. Since the rate of electrocatalysis depends primarily on the formal redox potential difference of the catalyst and analyte, selectivity can be tuned by selecting the proper catalyst [49].

One of the most interesting properties of conducting polymers is their ability to catalyze some electrode reactions. A thin layer of a conducting polymer, deposited onto the surface of substrate electrode, is able to enhance the kinetics of electrode processes of some solution species. These electrocatalytic processes, proceeding at conducting polymer electrodes, present a fast growing area of investigation, which may yield many unexpected applications in various fields of applied electrochemistry.

At conducting polymer modified electrodes, at least three processes should be considered during electrocatalytic conversion of solution species.

1. A heterogeneous electron transfer between the electrode and a conducting polymer layer
2. Electron transfer within the polymer film. As usual, this process is accompanied by the movement of charge compensating anions and solvent molecules within the conducting polymer film, and
3. Possible conformational changes of polymer structure.

The rate of the first process is determined by many factors. Among these, the electrical conductivity of a polymer layer, electron self-exchange rate between the chains and or clusters of polymer, and anion movement within polymer film seem to be of great importance. The second process is the diffusion of solution species to the reaction zone, where the electrocatalytic conversion occurs. As compared to simple electrode reactions, this process can be more complicated in cases where the electrocatalytic conversion occurs within the polymer film. Then, the diffusion of species within the film, as well as the possible electrostatic interaction of this species with the polymer film should be taken into account and lastly, a chemical heterogeneous reaction takes place between solution species and conducting polymer.

From both theoretical and practical points of view, the question on the location of electrocatalytic process seem to be of primary interest. If the charge transfer within the layer of conducting polymer proceeds much faster than the mass transfer of reacting species and their electrochemical conversion, the electrocatalytic process should proceed at the outer conducting polymer solution interface. In an opposite case, if the mass transfer and electrochemical reaction proceed faster than the electron transfer in conducting polymer, an electrocatalytic process occurs at the inner substrate electrode conducting polymer interface, assuming that the permeability of a porous conducting polymer layer is sufficient high to penetrate the reacting species and solution ions. At last, if both above processes occur at a comparable rate, the electrocatalytic process is located within the conducting polymer layer. The depth of the reaction zone within the conducting polymer layer will be determined in this case by the balance between charge and mass transfer, and the rate of electrocatalytic conversion as well. The problem on the location of electrocatalytic process is often considered as the question on either metal-like electrocatalysis at conducting polymer solution interface,

or semiconductor-like electrocatalysis either within the polymer layer, or at inner substrate electrode conducting polymer interface.

### 2.8 Detection of hydroquinone, catechol and ascorbic acid

Hydroquinone (1,4-dihydroxybenzene) (Fig. 3a) and catechol (1,2-dihydroxybenzene) (Fig. 3b) are phenolic compounds and often coexist as isomers in environmental samples. Simultaneous determination of hydroquinone and catechol levels is of great importance because of their coexistence in environmental samples as environmental pollutants with high toxicity. Most established common methods for the determination of catechol and hydroquinone are performed after previous separation [50]. Disadvantages of the separation are operating complexity, time wastage and reagent consumption. Thus, it is necessary to develop a new method with possibility of the simultaneous determination without previous separations of these compounds. Both hydroquinone and catechol have a basic quinone structures that may be electrochemically oxidized at a platinum or carbon electrodes. A simultaneous investigation of electrochemical behavior of hydroquinone and catechol was suggested at a poly(5-sulfosalicylic acid) modified electrodes with 105 mV of potential difference between the oxidation peak of hydroquinone and the oxidation peak of catechol [51] and multiwall carbon nanotube (MWNT) modified electrode with 102 mV potential difference between the oxidation peak of hydroquinone and the oxidation peak of catechol [50].

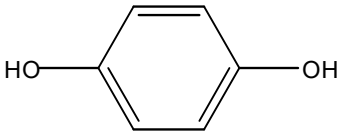


(a) Hydroquinone

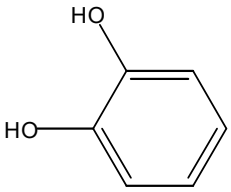


(b) Catechol

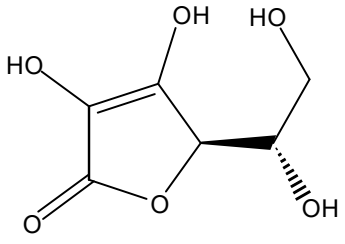


(c) Ascorbic acid

Figure 3. Chemical structures of hydroquinone, catechol and ascorbic acid

One of the redox systems most often used in the investigation of electrocatalysis at conducting polymer electrodes is the hydroquinone/benzoquinone redox couple (HQ/BQ). The well studied quasireversible redox transition between HQ and BQ implies the transfer of two electrons and two protons, in acidic aqueous solutions. However, at high pH, and in non aqueous solutions, intermediate products like anion radicals, are known to form during the electrochemical oxidation or reduction. Cooper and Hall [52] found the reduction of BQ proceeds nearly reversibly with $2e^-$ transfer at stationary polyaniline electrodes in the low pH region, whereas the transfer of the second electron is prevented at rotating disc electrode by the loss of intermediate from the surface before it can migrate into the polymer film. The authors concluded that, at stationary electrode, the reaction product is stabilized by the possible formation of the charge compensating complex between BQ anion radical and the polymer. At higher pH, the reaction occurs on the outside of PANI film, because of the slow charge transfer through the polymer film.

Measuring the secretion of neurotransmitters such as catechol and catecholamine has been considered to be of great importance to probe the brain chemistry. Many researches carried out a research to detect catechol [50, 53] where the major difficulty in electrochemical detection of this neurotransmitter was the interference from excess ascorbic acid (Fig. 3c), which oxidizes at the same potential as catechol. Ascorbic acid is a most common electroactive compound in biological compounds. It is used as an additive to prevent color, aroma and flavor change in foods using its reducing and antioxidant property. It also has clinical importance, e.g., prevention of scurvy and is vital to immune response and wound healing. Recently, the anticancer and antitumor properties of organometallic ascorbic acid were also investigated [54]. As a result considerable attention was paid in recent years to conducting polymer electrode assisted electroanalysis of ascorbic acid (vitamin C) in biological liquids. Protiva Rani Roy *et al.* [54] showed the glassy carbon electrodes, covered with electropolymerized layer of N, N-dimethylaniline exhibit electrocatalytic properties towards the oxidation of ascorbic acid. Others used polythiophene derivative redox polymer modified Pt electrode for electrocatalytic oxidation of ascorbic acid [55]. The determination of catechol in the presence of ascorbic acid has attracted the interest of many researchers.

## 3. EXPERIMENTAL SECTION

### 3.1. Solution Preparation

0.1 M Lithium perchlorate ($LiClO_4$) (Aldrich) in acetonitrile (Riedel-Dehaen) was used as a supporting electrolyte. 0.25 M of monomers 3-hexylthiophene (Aldrich), 3-methylthiophene (aldrich) and 3-octylthiophene dissolved in 0.1 M $LiClO_4$ - acetonitrile solutions were used in the electrochemical polymerization. 1 M phosphoric acid ($H_3PO_4$) (Riedel-Dehaen) and 0.1M sodium hydroxide (NaOH) (BDH) were used for varying the pH of the phosphate buffer solutions (mixture of disodium orthophosphate ($Na_2HPO_4.12H_2O$) (BDH) and sodium dihydrogen orthophosphate ($NaH_2PO_4.2H_2O$) (BDH)), and 1M potassium nitrate ($KNO_3$) (BDH), were used as supporting electrolytes during the electrochemical characterization of the electrocatalytic effect of the polymers and copolymers formed on the working electrode. The analytes used in the aqueous system were potassium ferricyanide ($K_3Fe(CN)_6$) (BDH), ascorbic acid ($C_6H_8O_6$) (Hopkin and Williams Ltd.), catechol ($C_6H_4(OH)_2$ ) (Aldrich) and hydroquinone ($C_6H_4(OH)_2$ ) (May and Baker Ltd)

### 3.2. Preparation of electrodes

#### 3.2.1. *Reference Electrodes*

The reference electrode used in organic solutions was quasi Ag/AgCl reference electrode. It was prepared by applying a potential of 4.60 V from a dc source between silver and a platinum wire immersed in a saturated potassium chloride solution. In aqueous solutions commercial standard Ag/AgCl reference electrode was used.

#### 3.2.2. *Counter Electrodes*

Platinum foil in organic solutions and Pt wire in aqueous solutions were used as counter electrodes. These electrodes were cleaned using a blue flame from Bunsen burner.

#### 3.2.3. *Working Electrodes*

Unmodified (bare electrodes) and modified platinum disc electrodes in the study of monomers and polymers in organic solutions were used. The unmodified electrodes were platinum disc (2 mm diameter), gold disc electrode (2 mm diameter), glassy carbon (GC) disc electrode (3 mm diameter), from CH Instruments and indium doped tinoxide coated on glass (ITO) were

used. Except ITO, the working electrodes were polished with alumina (0.05 micron) powder to a mirror finish in every experiment. The ITO electrode was successively cleaned with deionized water, acetone and isopropanol or ethanol.

The working electrodes in the electrocatalytic studies were bare platinum disc or platinum disc electrode modified with copolymers of: 3-methylthiophene and 3-octylthiophene, 3-hexylthiophene and 3-octylthiophene, and homopolymers poly(3-methylthiophene), and poly(3-octylthiophene).

Prior to the modification, the surface of the polished Pt electrode was sonicated with deionized water for 10 minutes to remove the alumina from the surface of the electrode and then dried with an air gun. The electrochemical polymerization was carried out potentiostatically at a potential of 2.00 V for 10 seconds. After electrochemical deposition of the polymer on the electrode surface it was removed from the monomer solution and rinsed with acetonitrile and deionized water successively. The elctrode was then dipped in to 0.1 M aqueous phosphate buffer solution (pH 4.0) for ascorbic acid /catechol detection and in 0.3 M aqueous phosphoric acid solution (pH 0.5) for hydroquinone/catechol detection. The potential was scanned between –0.20 V and 0.80 V in the absence of the analyte until a stable background was obtained usually for 21 cycles.

### 3.3 Experimental Setups and Procedure

All the electrochemical polymerization and electrochemical characterizations were carried in a three-electrode one-compartment electrochemical cell. An electrochemical analyzer (BAS CV-50W) was used to run all electrochemical experiments. The pH measurements were carried using PH/ION meter level 2. All potentials are reported *versus* Ag/AgCl reference electrode. Before each experiment was carried the solutions were purged with a stream of argon and blanketed with argon throughout the experiment.

Before electrochemical polymerizations and characterizations the appropriate working potential window was selected using the supporting electrolyte solution. Then the electrochemical behavior of the monomers, homopolymers and copolymers were studied.

Finally the electrocatalytic behavior of the polymers and copolymers were studied on selected biological and environmental samples.

To run thermal analysis experiments (Differential Scanning Calorimetric, DSC) a thermal analyzer (SDT Q6000 V3.8 Build 51) was used.

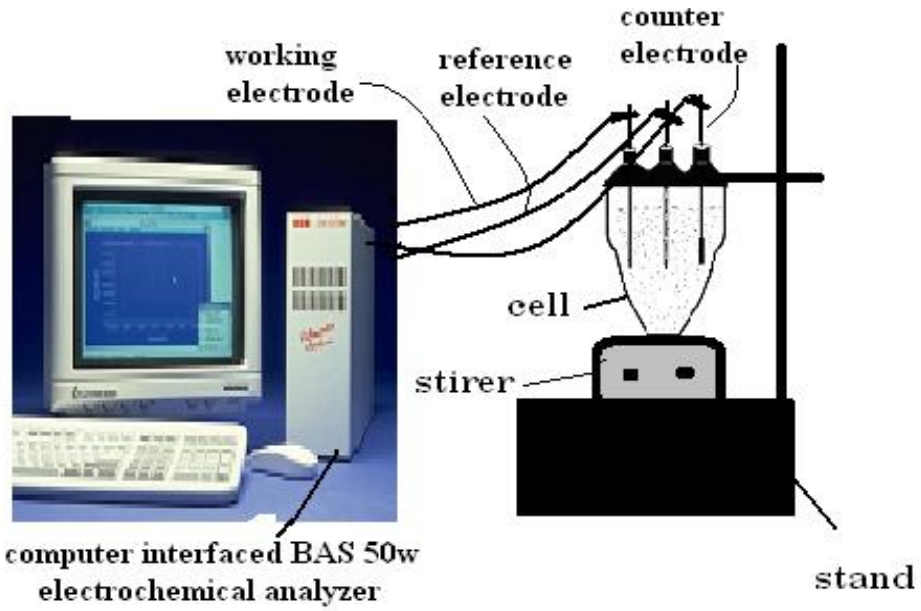


Figure 4. General experimental setup used for the electrochemical studies.

## 4. RESULTS AND DISCUSSION

### 4.1. Electrochemical Studies

The electrochemical potential windows of the supporting electrolyte (0.1 M $LiClO_4$ - acetonitrile) solution were examined before the electrochemical polymerization and characterizations were carried at different working electrodes (Pt, Au, GC and ITO) using cyclic voltammetry. There were no other interfering electrochemical reactions within the potential ranges where the monomers and polymers were electrochemically studied.

Once the appropriate potential window was known the electrochemical behavior of the monomers 3-hexylthiophene (3HT) and 3-octylthiophene (3OT) and the homopolymers were examined. The cyclic voltammograms for the different monomers at various electrodes are depicted in Figures 5 and 6.

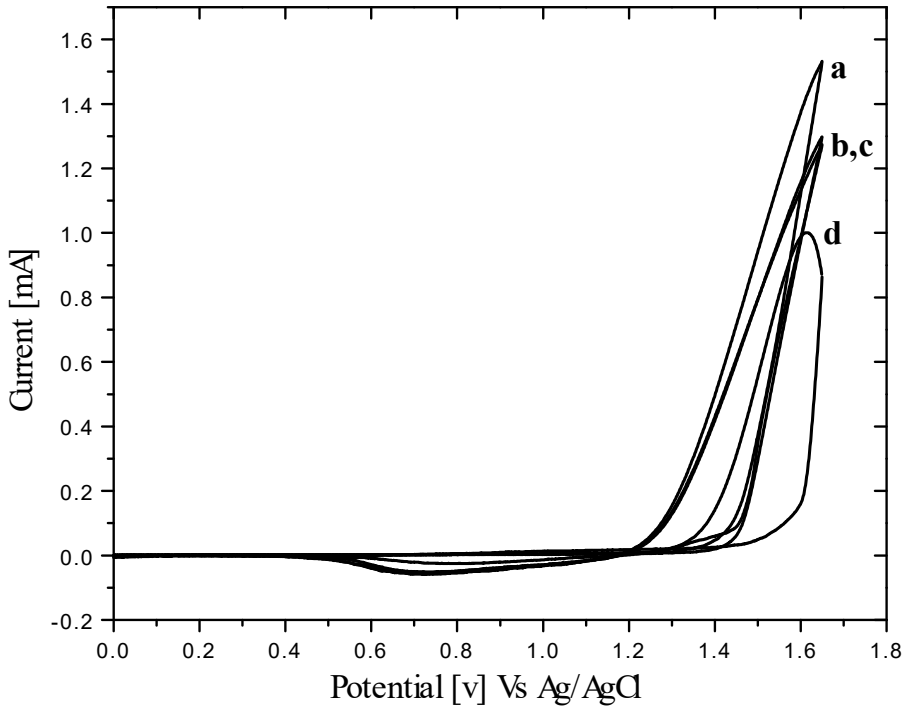


Figure 5. Cyclic voltammogram for the monomer 0.25 M 3HT in 0.1 M $LiClO_4$ - acetonitrile solution at a) GC, b) Au, c) Pt, d) ITO working electrodes, at a scan rate of 10 mV/s.

As can be seen from Figure 5 the onset oxidation potentials of 3HT is nearly the same for Pt, Au, and glassy carbon electrodes while there is a slight shift to a higher potential in case of ITO. This might be due to the weak adsorption effect of P3HT on the ITO surface as observed from electropolymerization of P3HT on ITO. It was noted that the electropolymerization on ITO surface was not possible for 3HT. The higher current response at glassy carbon (GC) than the response at gold and platinum was due to the difference in surface area of the electrodes. The low current response at ITO again confirmed the weak adsorption of P3HT on ITO although its surface area was larger than that of Au, Pt and GC electrodes.

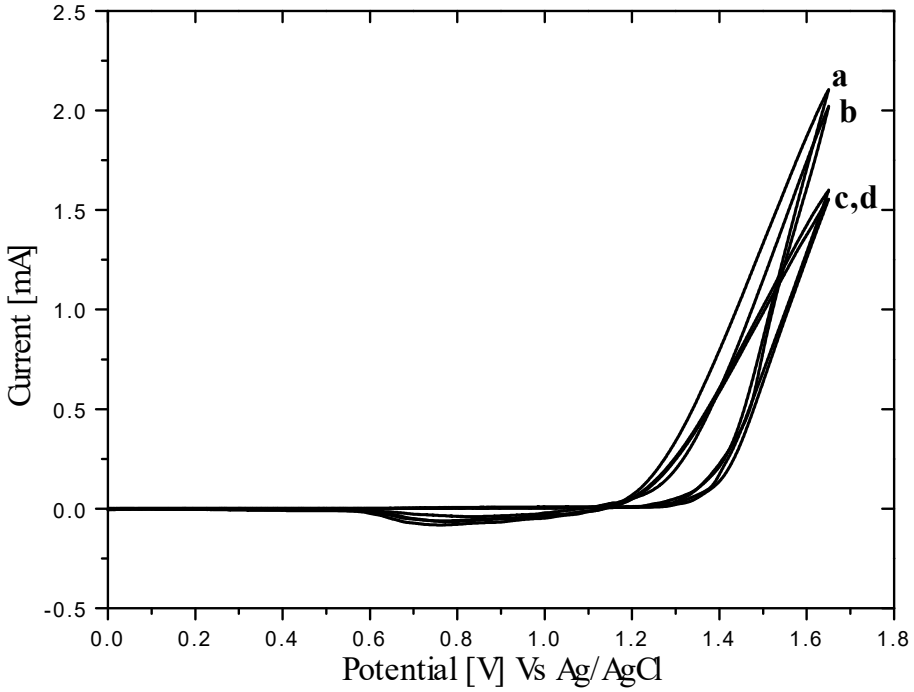


Figure 6. Cyclic voltammogram for the monomer 0.25 M 3OT in 0.1 M $LiClO_4$ - acetonitrile solution at a) ITO, b) GC, c) Au, d) Pt working electrodes, at a scan rate of 10 mV/s.

In the case of 3OT (Fig. 6) no significant differences in oxidation onset potentials of the monomer were observed at the various electrodes. The variation in current response was observed due to the difference in surface areas of the electrodes. In this case the higher current response at ITO electrode is indication of the difference in adsorption of P3HT and P3OT on ITO. When the onset oxidation potentials of the two monomers are compared, 3OT oxidizes

at a higher potential than 3HT except on ITO electrode. This variation is clearly observed when using Pt electrode as shown in Figure 5. The onset for oxidation of 3HT is at 1.50 V while that of 3OT is at 1.55 V. The lower oxidation potential and the higher current response of 3HT indicate that 3HT is oxidized easily than 3OT.

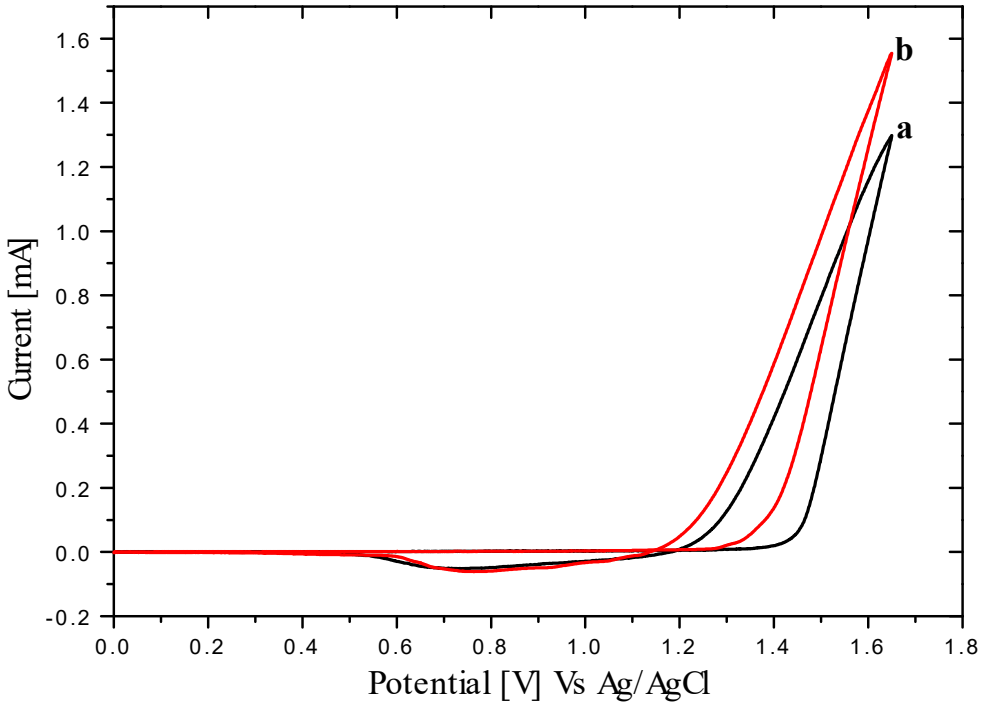


Figure 7. Cyclic voltammogram for the monomers 0.25 M 3HT and 0.25 M 3OT in 0.1 M $LiClO_4$ - acetonitrile solution at a Pt working electrode a) 3HT, b) 3OT at a scan rate of 10 mV/s.

Having the onset oxidation potentials of each monomer, the homopolymers of both 3HT and 3OT were produced by sweeping the potential from 0 V to 1.65 V. To see the effect of the electrodes on the oxidation potentials of the homopolymers the redox characteristics of the polymers were examined on Pt, Au and GC electrodes during the polymerization (polymer growth process) (Fig. 8 and 10) and in a monomer free electrolyte solution (Fig. 9 and 11).

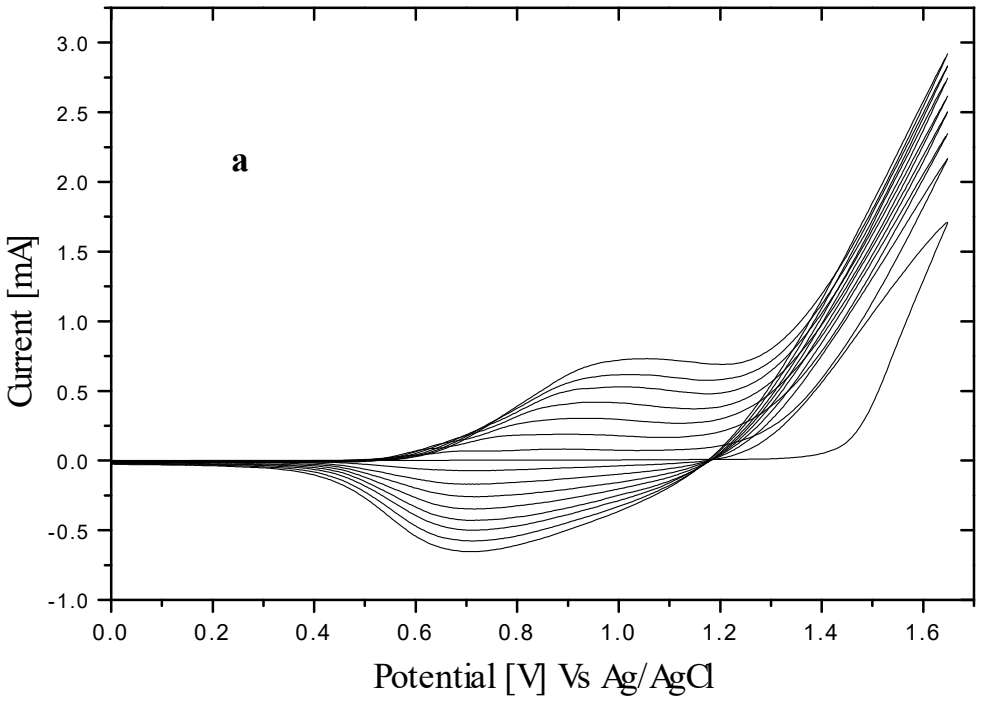
a
Current [mA]
Potential [V] Vs Ag/AgCl
3.0
2.5
2.0
1.5
1.0
0.5
0.0
-0.5
-1.0
0.0
0.2
0.4
0.6
0.8
1.0
1.2
1.4
1.6

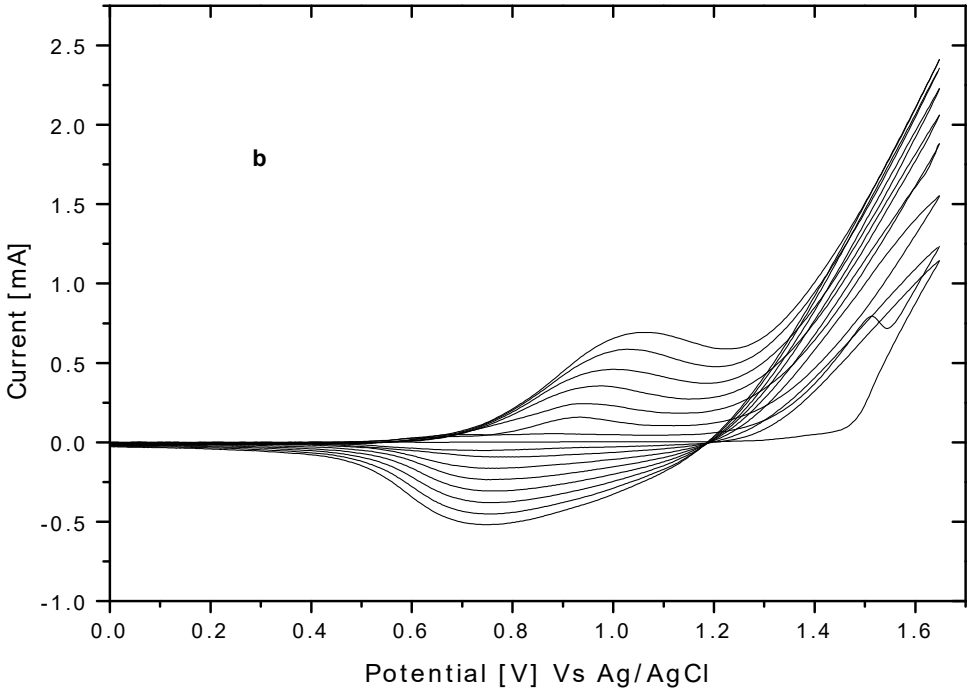
b
Current [mA]
Potential [V] Vs Ag/AgCl
2.5
2.0
1.5
1.0
0.5
0.0
-0.5
-1.0
0.0
0.2
0.4
0.6
0.8
1.0
1.2
1.4
1.6

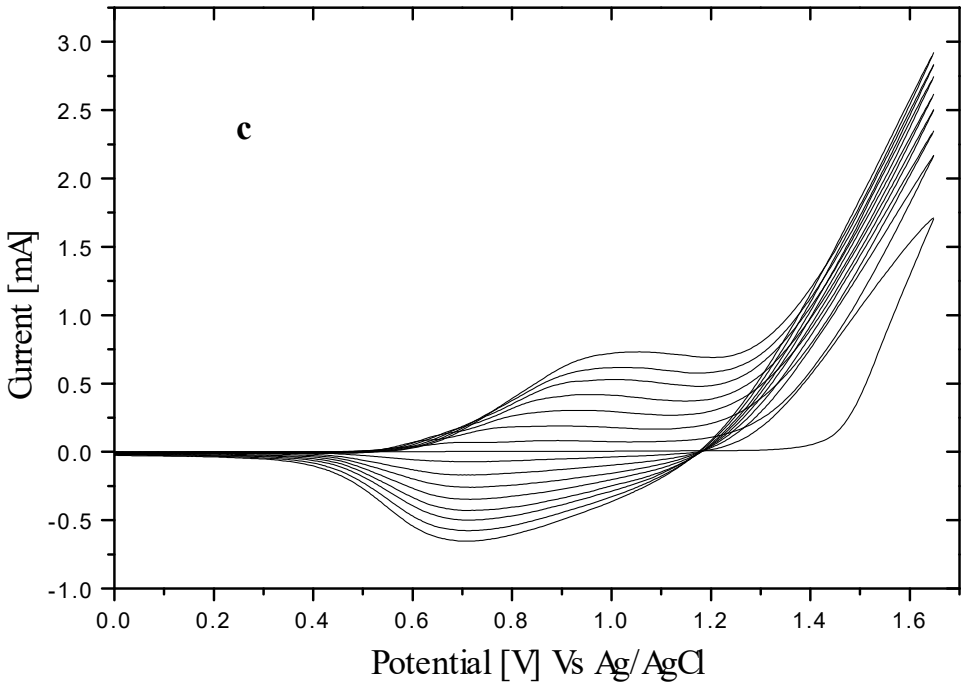


Figure 8. Cyclic voltammograms of polymerization of 0.25 M 3HT in 0.1 M $LiClO_4$ - acetonitrile solution at a) GC b) Au c) Pt working electrodes, at a scan rate of 10 mV/s.

From the shape of the cyclic voltammogram of the polymerization of 3HT for the successive 16 cycles run, an increase in oxidation peak current in the three electrodes was observed, which indicates that there is a film growth after each cycle on each electrode. For all electrodes oxidation onset potential for the first scan was higher than for the second and for higher scans (Fig. 8 a, b, c). There are two possible reasons for this; the first reason is that the monomer might easily be oxidized on the polymer film formed during the initial polymerization process as compared to bare electrodes. The second reason is that the oligomers formed during the first scan remaining in the solution could reduce the apparent potential of the monomer oxidation; this is because oligomers are known to be oxidized at lower potentials than their corresponding monomers [31]. This indicates an electrocatalytic effect of the polymer films on oxidative polymerization of their respective monomers.

When the redox behavior of the P3HT was examined in a monomer free solution a slight difference in the oxidation potentials were observed at different electrodes (1.14 V at glassy carbon, 1.15 V at gold electrode and 1.17 V at a platinum electrode) (Fig.9). This might be due to the difference in the amount of adsorption of P3HT film on the electrode surfaces and also might be because of differences in work functions of the three electrodes (5.64 eV for Pt, 5.10 eV for Au and 4.8 eV for GC) [31].

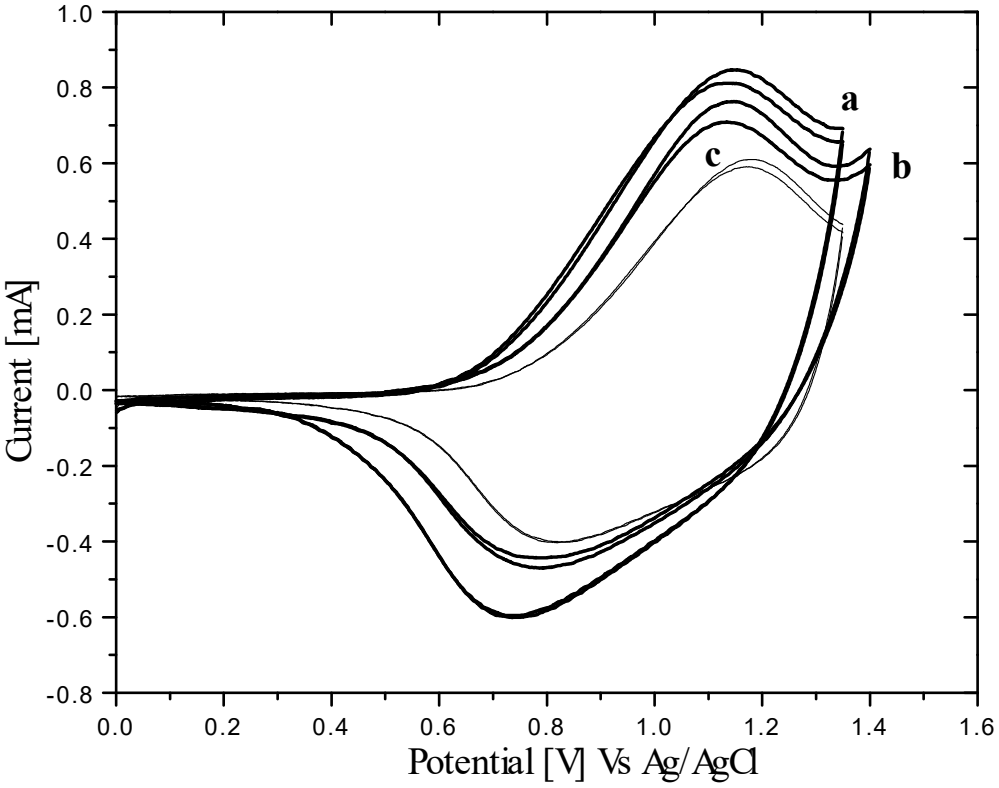


Figure 9. Cyclic voltammogram of P3HT in monomer free 0.1 M $LiClO_4$ - acetonitrile solution, polymerized by scanning 0.25 M 3HT at a) GC b) Au c) Pt working electrodes, at a scan rate of 10 mV/s.

Similar observations were made for 3OT (Fig. 10a, b, c) as that of 3HT. The position of the oxidation onset potential of the monomer during the growth of the polymer P3OT was different between the first scan and the successive scans. However there was a difference in the position and shape of the cyclic volammogram during the growth of the polymer for P3OT on glassy carbon electrode and the other two electrodes (Pt and Au).

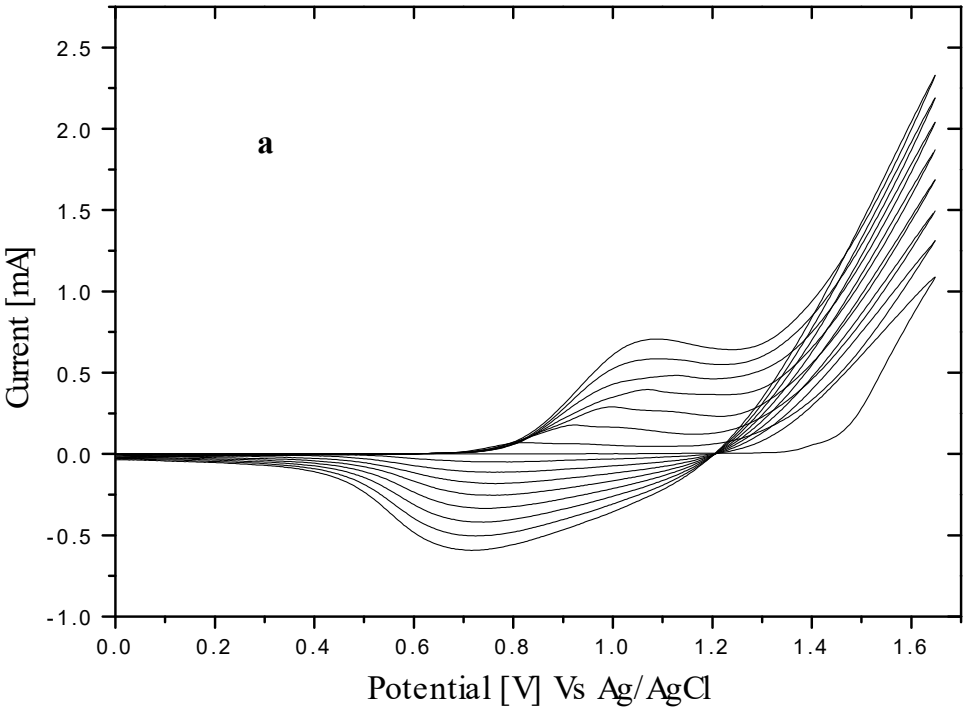
a
Current [mA]
Potential [V] Vs Ag/AgCl
2.5
2.0
1.5
1.0
0.5
0.0
-0.5
-1.0
0.0
0.2
0.4
0.6
0.8
1.0
1.2
1.4
1.6

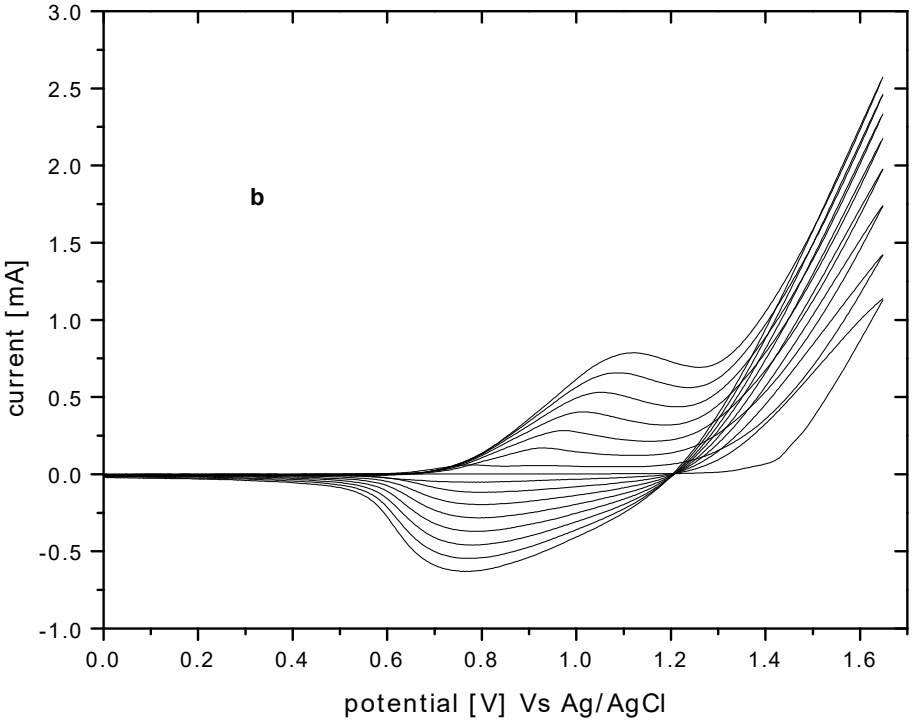
b
current [mA]
potential [V] Vs Ag/AgCl
3.0
2.5
2.0
1.5
1.0
0.5
0.0
-0.5
-1.0
0.0
0.2
0.4
0.6
0.8
1.0
1.2
1.4
1.6

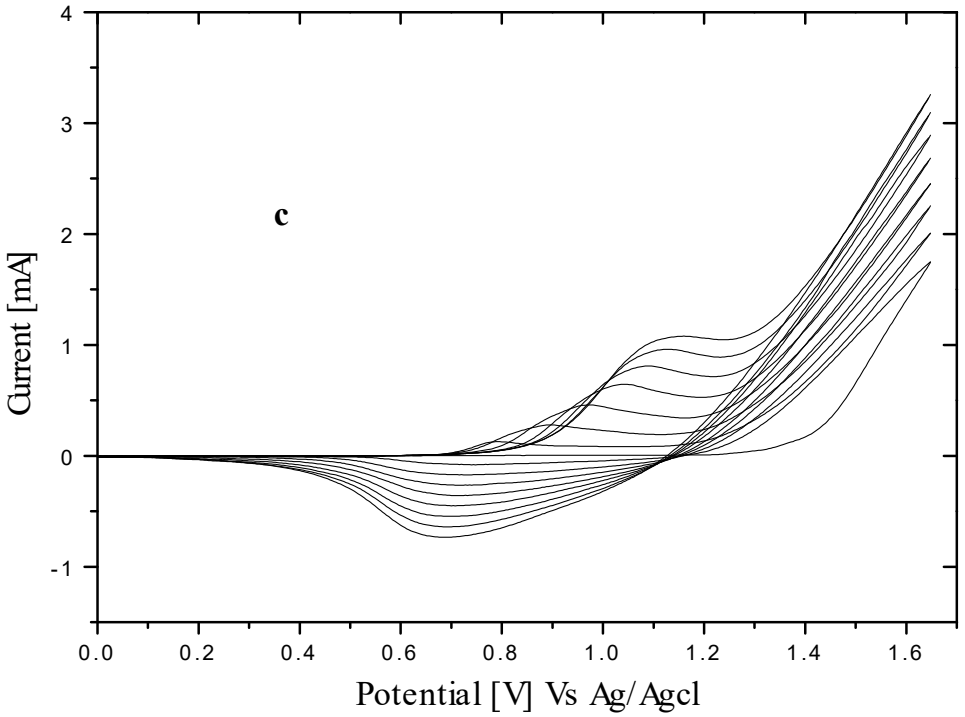


Figure 10. Cyclic voltammograms of polymerizations of 0.25 M 3OT in 0.1 M $LiClO_4$ - acetonitrile solution at a) Pt b) Au c) GC working electrodes at a scan rate of 10 mV/s.

Comparison of the polymerization of the two monomers shows that (Fig. 8 and 10), the oxidation potential of 3OT is higher than that of 3HT. This indicates the ease of oxidation of 3HT, as reported in literature [56]. It was also noted that cyclic voltammogram of P3HT during the growth of the polymer covers broader oxidation potential range when using GC, Au and Pt electrodes. This was not the case for P3OT, where the corresponding voltammograms of electrochemical polymerization showed relatively sharper oxidation. This indicates that P3HT is more conductive in wider range of potentials than P3OT in its oxidized form.

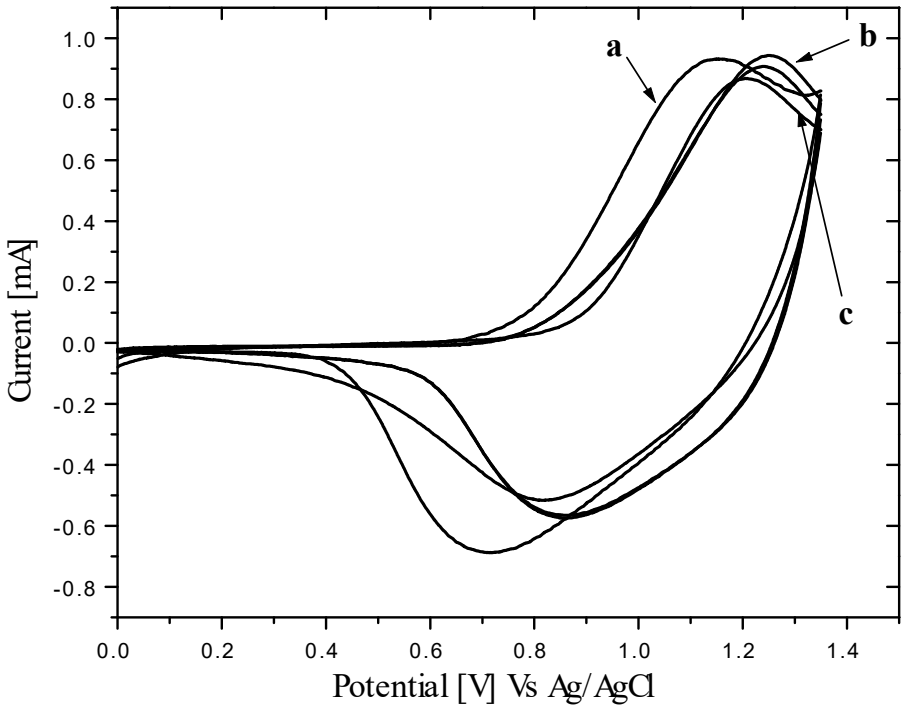


Figure 11.Cyclic voltammograms of P3OT in monomer free 0.1 M $LiClO_4$ - acetonitrile solution polymerized by scanning 0.25 M 3OT, at a) GC b) Au c) Pt working electrodes, at a scan rate of 10 mV/s.

The behavior of P3OT in monomer free solution at the three electrodes showed that oxidation peak potential of P3OT was significantly varied, 1.15 V at glassy carbon, 1.24 V at platinum and 1.20 V at gold electrode (Fig. 11). This shift in redox potential of the polymer films may be associated with the work function differences and the adsorption behavior (highly adsorbed on glassy carbon) of the polymer on the electrode surfaces.

When the redox behaviors of the two homopolymers were examined at a platinum electrode a significant difference between P3HT and P3OT was observed. As can be seen in Figure 12 the oxidation peak potential of P3OT is at 1.15 V and that of P3HT is at 0.97 V vs Ag/AgCl. Eventhough the potential variation seems small the properties of the two polymers are different in film formation.

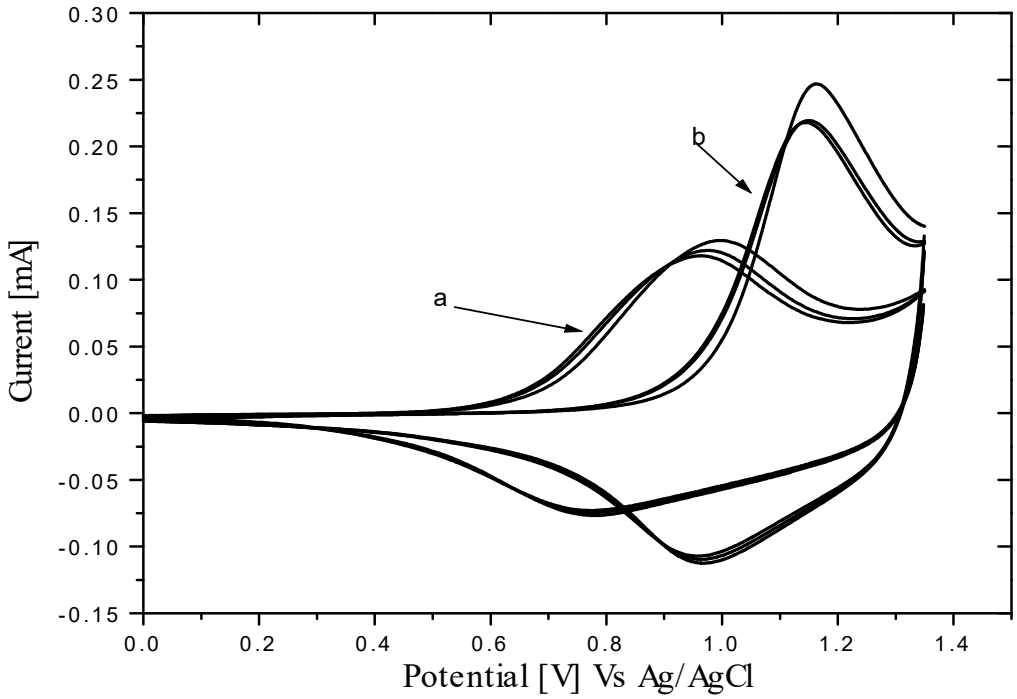


Figure12. Cyclic voltammograms of a) P3HT and b) P3OT in monomer free 0.1 M $LiClO_4$-acetonitrile solution polymerized by scanning 0.25 M of 3HT and 0.25 M 3OT at Pt working electrode, at scan rate of 10 mV/s.

In the case of P3HT no film was observed on transparent ITO electrode except some blue colored droplet like products, which later on pilled off and enter into the bulk of the solution. This property makes the determination of its optical absorption very difficult on ITO, whereas P3OT has good film forming property on ITO and on the other electrodes. On ITO electrode P3OT showed a deep blue transparent film during oxidation and, changed its color to red brown in its reduced neutral state. In addition, P3OT has shown a sharper peak than P3HT during oxidation and reduction. Sharpness is associated with symmetric arrangement of monomers in the polymer [37]. This indicates that the arrangement of 3OT is relatively symmetric than that of 3HT in their respective polymers.

### 4.1.1 A Copolymer from 3-Hexylthiophene and 3-Octylthiophene

After examining the properties of the homopolymers, P3HT and P3OT, the synthesis and characterization of the copolymer of 3HT and 3OT was done by varying the monomer composition in the mixture and the polymerization potentials. The properties of the resulting polymers were compared with the homopolymers. This was done to confirm whether the newely synthesized polymer was the coplymer of 3HT and 3OT or not. Table 1 summarizes the data obtained from the synthesis at different volume ratios of the two monomers and at varied polymerization potentials. The most appropriate volume ratio of the monomers was found to be 1:1.5 at a potential of 1.70 V. The oxidation potential of the copolymer is between the two homopolymers prepared potentiostatistically at the given potentials.

Table.1. The oxidation peak potentials, $E_{pa}$, of copolymers prepared from different monomer volume ratios of 0.25 M 3HT and 3OT at different potentials potentiostatically, with a scan rate of 10 mV/s.

| P3HT | | P3OT | | poly(3HT-co-3OT) | | | | | |
|---|---|---|---|---|---|---|---|---|---|
| | | | | 1:1 ratio | | 1:1.5 ratio | | 1:2 ratio | |
| E | $E_{Pa}$ | E | $E_{Pa}$ | E | $E_{Pa}$ | E | $E_{Pa}$ | E | $E_{Pa}$ |
| 1.55 | **0.934** | 1.60 | **0.985** | 1.60 | 0.937 | 1.60 | 0.955 | 1.60 | 0.969 |
| | | | | 1.65 | 0.948 | 1.65 | 0.957 | 1.65 | 0.972 |
| | | | | 1.70 | 0.956 | **1.70** | **0.960** | 1.70 | 0.993 |
| | | | | 1.80 | 0.985 | 1.80 | 0.995 | 1.80 | 1.006 |

As can be seen from the voltammograms (Fig. 13) oxidation potential of the copolymer is at the intermediate position between oxidation potentials of the homopolymers, which generally shows that a polymer with a new property is produced. In addition when the copolymer was electrochemically polymerized on ITO electrode with 1:1.5 ratio of 3HT and 3OT at a potential of 1.7 V, it showed a good film forming properties with a color contrast of deep blue in oxidized state and red brown in the neutral state.

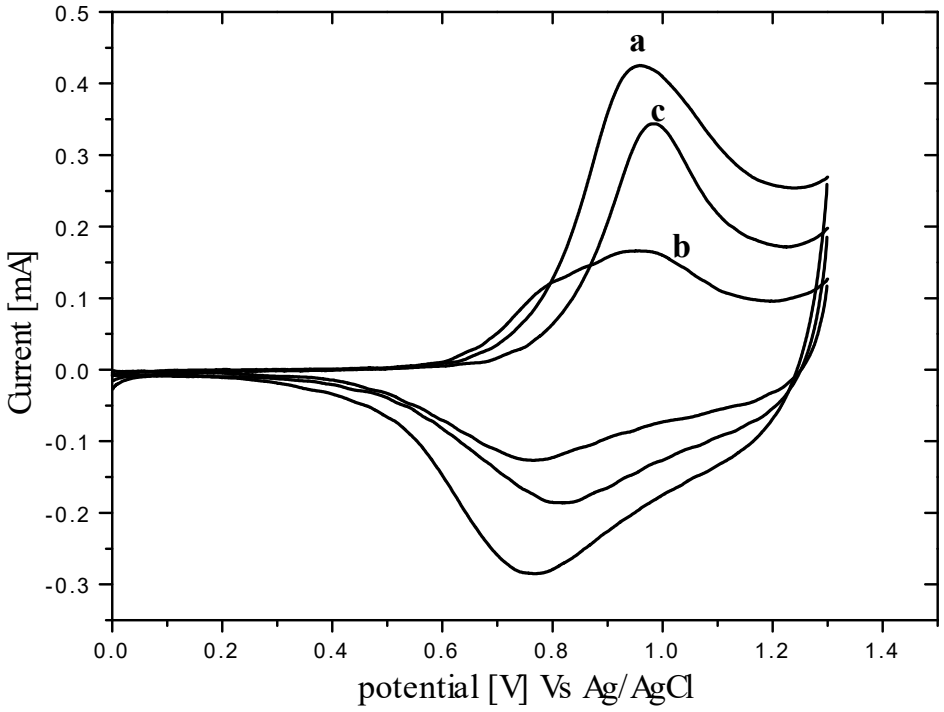


Figure 13. Cyclic voltammograms of (a) poly(3HT-co-3OT) elctropolymerized at 1.70 V from volume ratio of (1:1.5) 3HT to 3OT , (b) P3HT (c) P3OT elctropolymerized at 1.55 V and 1.60 V respectively, in a monomer free 0.1 M $LiClO_4$ - acetonitrile solution at a scan rate of 10 mV/s.

In a fixed monomer mixture with volume ratio of 1:1.5 of 0.25 M 3HT to 3OT the polymerization potentials was systematically varied between 1.60 V and 1.80 V expecting the resulting copolymer may have different ratios of each component in the copolymer. The cyclic voltammograms of the copolymers generated at different potentials are different from those of the homopolymers (Fig. 14). This shows that it is possible to prepare copolymers with different proportion of the monomers in the structure of the copolymer.

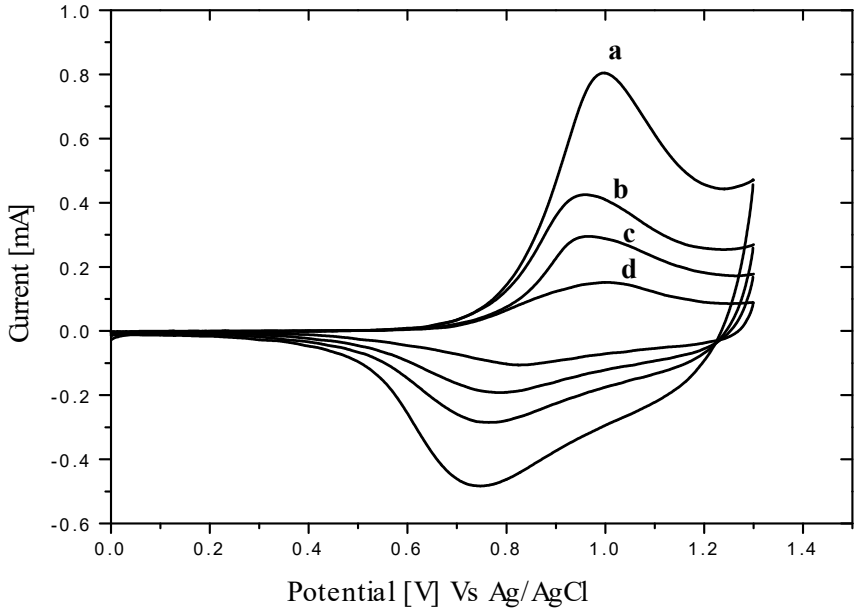


Figure 14. Cyclic voltammograms of different copolymers in a monomer free 0.1 M LiClO4-acetonitrile solution obtained from a volume ratio of 1:1.5 of 0.25 M 3HT to 3OT polymerized at (a) 1.80 V,(b) 1.70 V,(c) 1.65 V (d) 1.60V at scan rate of 10 mV/s.

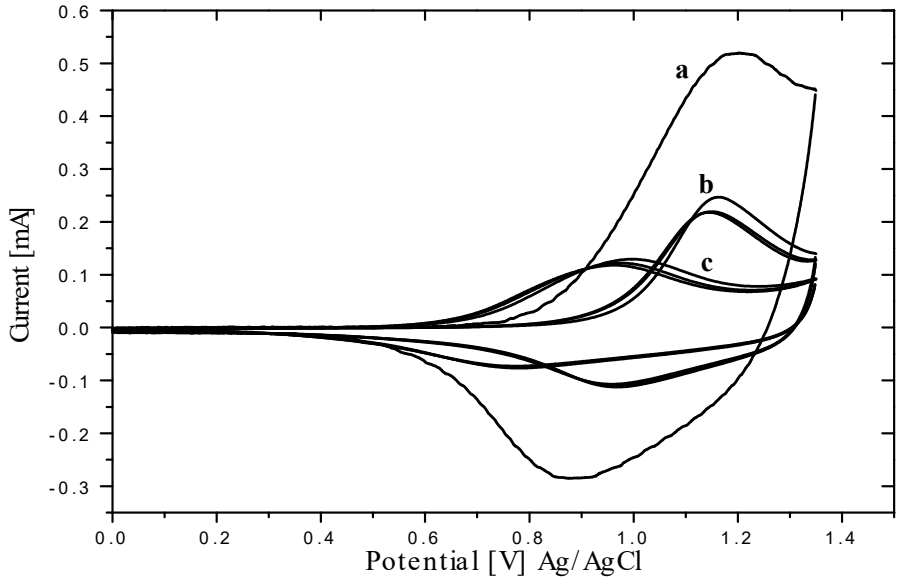


Figure 15. Cyclic voltammograms of (a) P3HT, (b) P3OT , (c) poly(3HT-co-3OT) obtained by scanning 0.25 M of 3HT and 3OT and their 1:1.5 volume ratio mixture respectively in 0.1 M $LiClO_4$-acetonitrile monomer free solution at Pt electrode, at a scan rate of 10 mV/s.

To see the effect of polymerization potentiostatically and potentiodynamically the potential of a 1:1.5 volume ratio of 3HT to 3OT were scanned between 0 V and 1.65 V and compared with the voltammogramms of the homopolymers obtained with the same potential scan (Fig.15). As can be seen from the Figure a copolymer is formed with in the same potential range. This is due to the closeness of the oxidation potentials of the two different monomers.

Finally the redox behavior of the copolymer was examined by scanning the potential with varying scan rates from 10 mV/s to 140 mV/s (Fig.16). As can be seen from the Figure redox behavior of the copolymer obtained showed an increase in anodic peak currents with scan

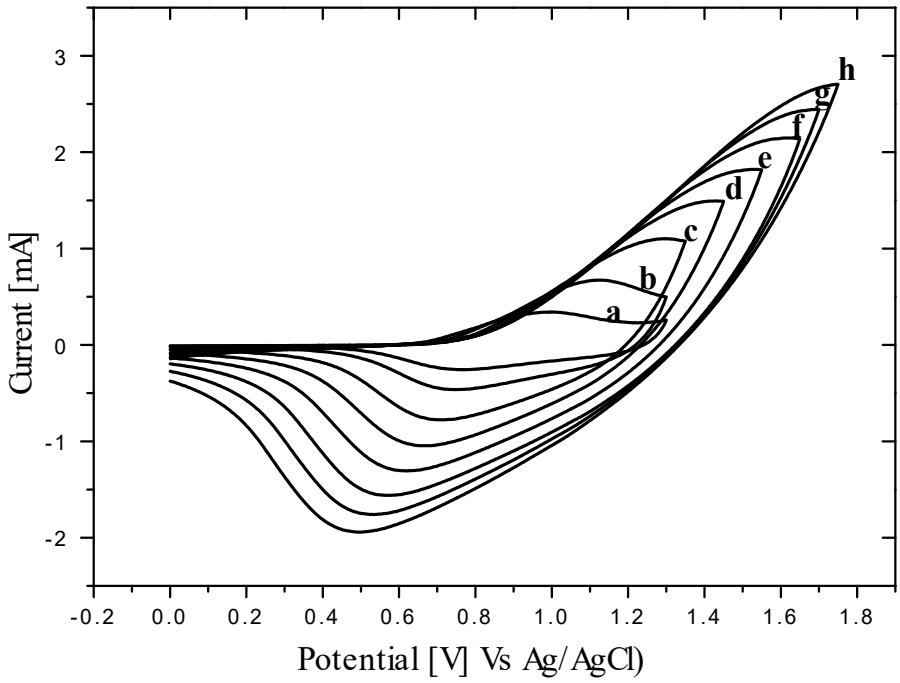


Figure 16.Cyclic voltammograms of poly(3HT-co-3OT) polymerized at 1.70 V in a monomer free 0.1M $LiClO_4$-acetonitrile solution at Pt electrode, with varying scan rates, (a)10 mV/s , (b) 20 mV/s and (h) 140 mV/s with 20 mV/s interval.

rate and a shift to a higher oxidation potential and a decrease in reduction potential of the copolymer with increasing scan rate, which is consistent with literature reports [28]. The oxidation peak current is linearly proportional to the scan rate as shown in Figure 17. This is the typical behavior of most conducting polymers adsorbed to an electrode surface [28, 57].

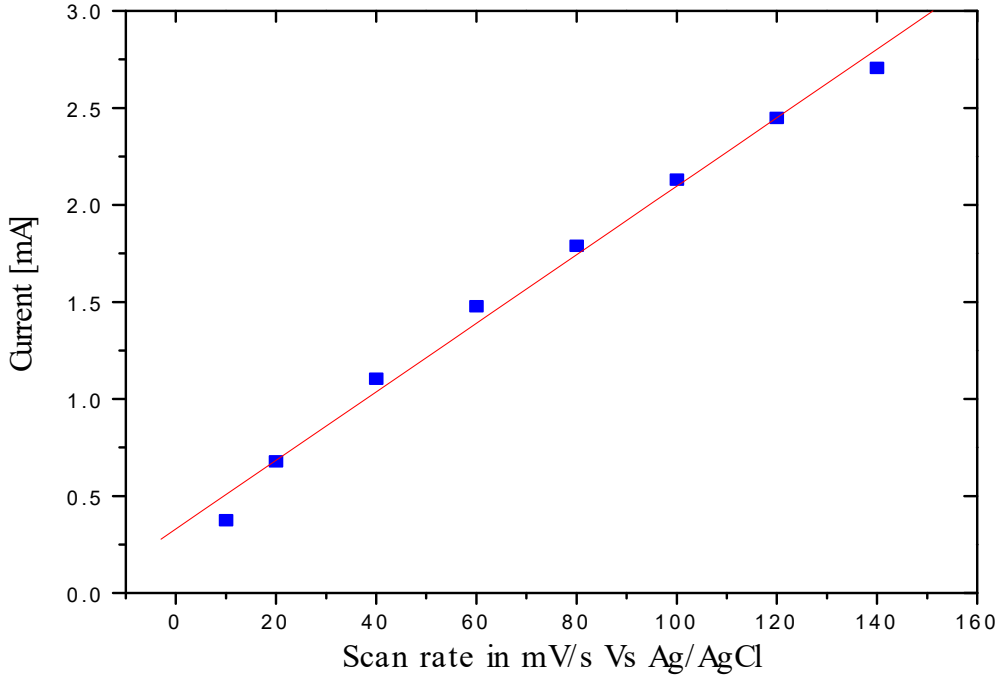


Figure 17. Dependence of oxidation peak current of poly(3HT-co-3OT) with scan rate in a monomer free 0.1 M $LiClO_4$-acetonitrile solution at Pt electrode,

#### 4.1.1.1 Thermal Analysis

The glass transition temperature ($T_g$ ) of a polymer is related to the thermal energy required to allow changes in the conformation of the molecules at a microscopic level. Above $T_g$ there is sufficient thermal energy for these changes to occur. Since the value of the glass transition temperature depends on the strain rate and cooling or heating rate, it is impossible to have an exact value for $T_g$. To determine the glass transition of the homopolymers and the copolymer Differential Scanning Calorimetry (DSC) experiments were carried at a scan rate of 10 $^0$C/min using the solid samples taken from the electrode surface after electrochemical polymerization of the polymers potentiostatically. From the DSC measurement (Fig.18) the glass transition temperatures of the polymers were 57.16 $^0$C for P3OT, 60.19 $^0$C for P3HT and 58.14 $^0$C for poly(3HT-co-3OT). This result confirms the formation of the copolymer because as the substitution of the alkyl chain increases the flexability of the polymer increases due to the occurrence of free volume, which makes the polymer easily flexible, and as a result the glass

transition temperature lowered. Therefore the glass transition temperature observed for the homopolymers and copolymer was in agreement with the literature value (trend) [56]. The glass transition temperature of the copolymer which is expected to consist of both hexyl and octyl substituents has values in between the $T_g$ of the two homopolymers.

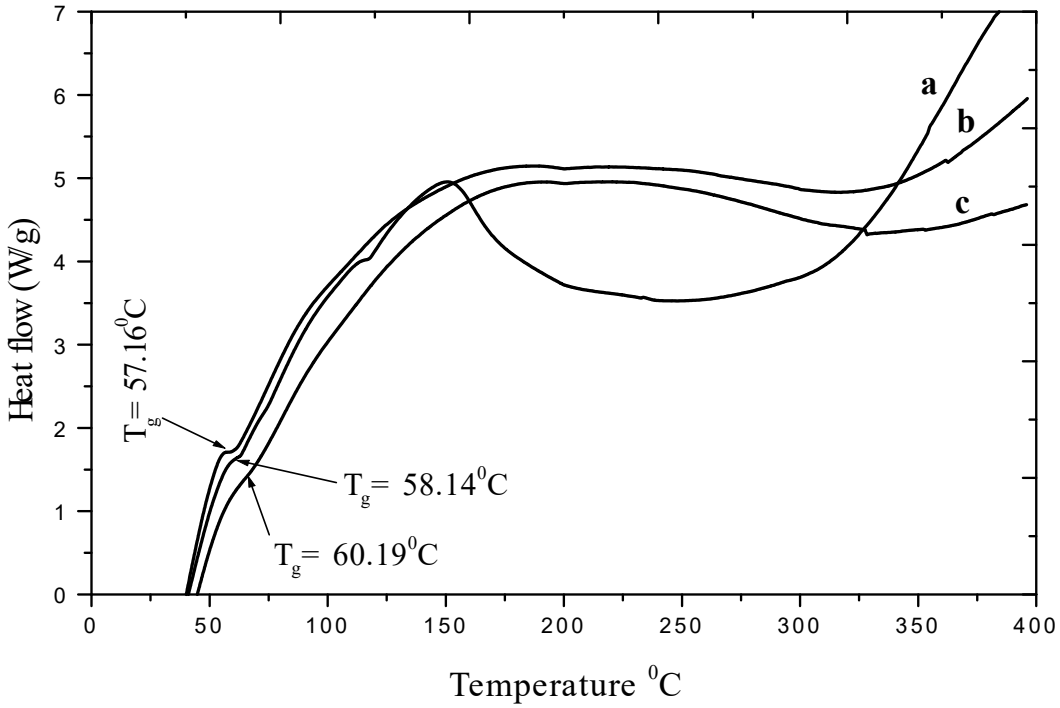


Figure 18. Differential Scanning Calorimetry of a) poly(3HT-co-3OT), b) P3OT and c) P3HT at a scan rate of 10 $^0$C/min.

### 4.1.2 A Copolymer from 3-Methylthiophene and 3-Octylthiophene

The other copolymer electrochemically synthesized and characterized was from 3-methylthiopene (3MT) and 3-octylthiophene (3OT). This is to use the advantage of high conductivity of P3MT [46] and the ease of polymerization and the sharpness of the oxidation of P3OT. As can be seen from Figure 19 the oxidation onset potentials of the monomers are 1.55 V for 3OT and 1.60 V for 3MT. The cyclic voltammogram of P3MT covers broader oxidation potential and no sharp oxidation peak was observed (Fig 20). This type of behavior is important if there is a need to have a polymer film with broad conductive potential range

where its oxidized state is conductive. It is known that P3MT has a conductivity of 43 S/cm in its oxidized state [58].

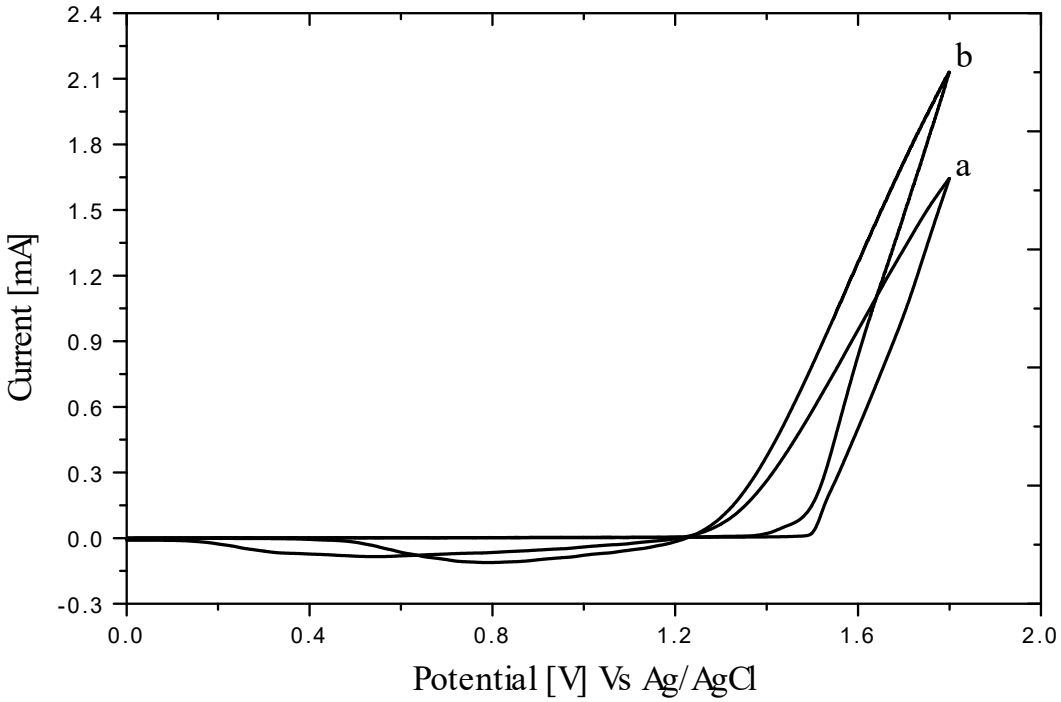


Figure 19.Cyclic voltammograms of the oxidation onset of a) 0.25 M 3MT, b) 0.25 M 3OT in 0.1 M LiClO4-acetonitrile solution at a Pt electrode, at a scan rate of 10mV/s.

Previous workers [39] showed that the molar ratio to have optimal copolymer formation from the two monomers is when the volume ratio is 1:2.5 (3OT: 3MT). Therefore in this work this ratio was used at a potential of 2.0 V to synthesize the copolymer electrochemically. The cyclic voltammogram of the homopolymers and copolymer produced are shown in Figure 21. As can be seen from the Figure the electrochemical behavior of P3MT is quite different from that of P3OT and P3HT. The oxidation peak of P3MT is at a lower potential than that of P3HT and P3OT.

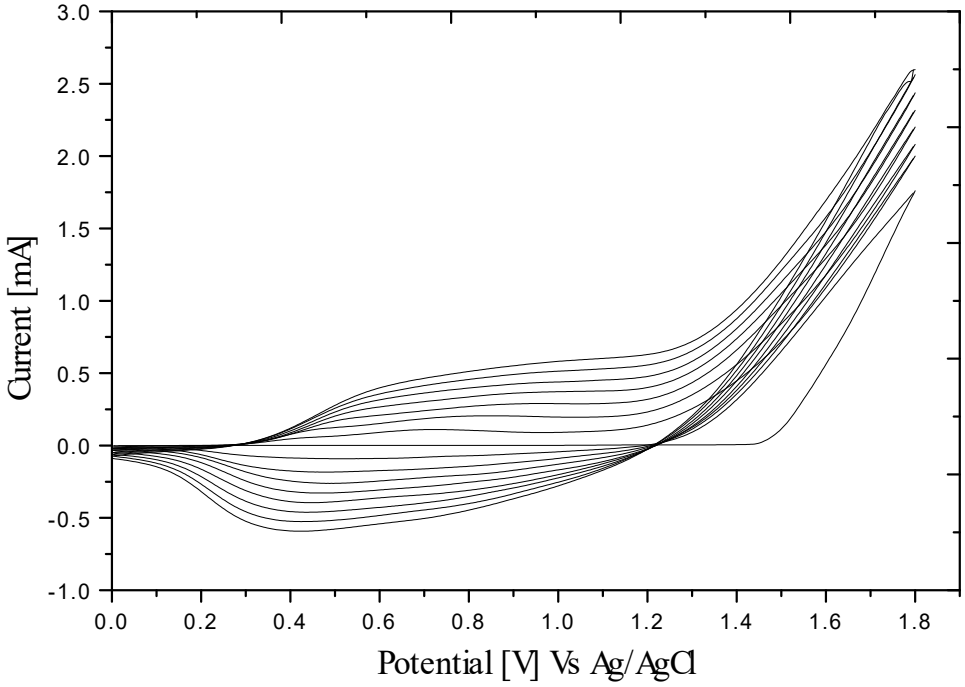


Figure 20. Cyclic voltammogram of polymerization of 0.25 M 3MT in 0.1 M $LiClO_4$-acetonitrile solution using Pt electrode at a scan rate of 10 mV/s.

However the oxidative polymerization of the monomer 3MT was at a higher potential than that of 3HT and 3OT (Fig.19). This indicates that the redox behaviors of the monomers are quite different from the corresponding polymers. The copolymer produced showed intermediate electrochemical property between P3MT and P3OT, and is expected to have a moderate conductivity in between the two homopolymers (Fig. 21).

From the cyclic voltammograms of the polymers P3MT, P3HT and P3OT (Fig.8-12 and Fig.19-21), it seems that there is a correlation between conductivity values of the polymers (43 S/cm for P3MT, 18 S/cm for P3HT and 15 S/cm for P3OT) [58] and the broadness of the oxidation potential during the growth of the polymer and in the monomer free solution. From this, it is possible to conclude that the broader the oxidation potential ranges the higher the conductivity of the polymer.

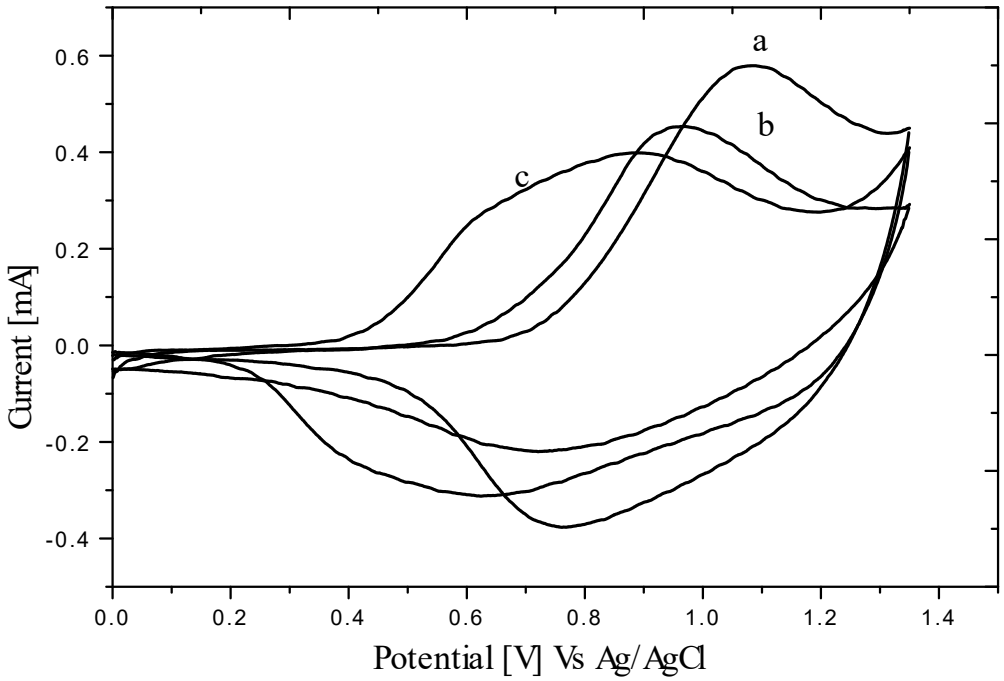


Figure 21. Cyclic voltammmogram of a) P3OT b) poly(3MT-co-3OT), c) P3MT, in 0.1 M $LiClO_4$-acetonitrile monomer free solution, at a scan rate of 10 mV/s.

Being able to produce the two copolymers; poly(3HT-co-3OT) and poly(3MT-co-3OT) and the two homopolymers; P3MT and P3OT their applications in the electrocatalysis of organic analytes were studied and presented in the section to follow.

## 4.2 Studies on Electrocatalysis at Conducting Polymer Electrodes

### 4.2.1 Voltammetric behavior of potassium ferricyanide at polymer modified Pt electrode

An electrode that is used to catalyze a reaction usually has a better redox current or selectivity. Such an electrode can be obtained by modifying with conducting polymers. Therefore, in this section the electrocatalytic properties of conducting polymer modified electrodes towards selected biological and environmental samples were examined and compared with the unmodified electrodes.

The first experiment carried was to check whether the polymers deposited at the electrode have an electrocatalytic effect on a given redox system. To see this a known redox system, 2 mM potassium ferricyanide, $K_3 Fe(CN)_6$, in 1 M aqueous potassium nitrate ($KNO_3$) was used. Furthermore the best electrocatalytic polymer was selected and the optimum thickness of the polymer that resulted in a high current response was determined by varying the deposition time during potentiostatic polymerization. Figure 22 shows the electrocatalytic effect of homopolymers and copolymers deposited for 10 s at a platinum electrode for the electrochemical reaction shown below in Equation 1.

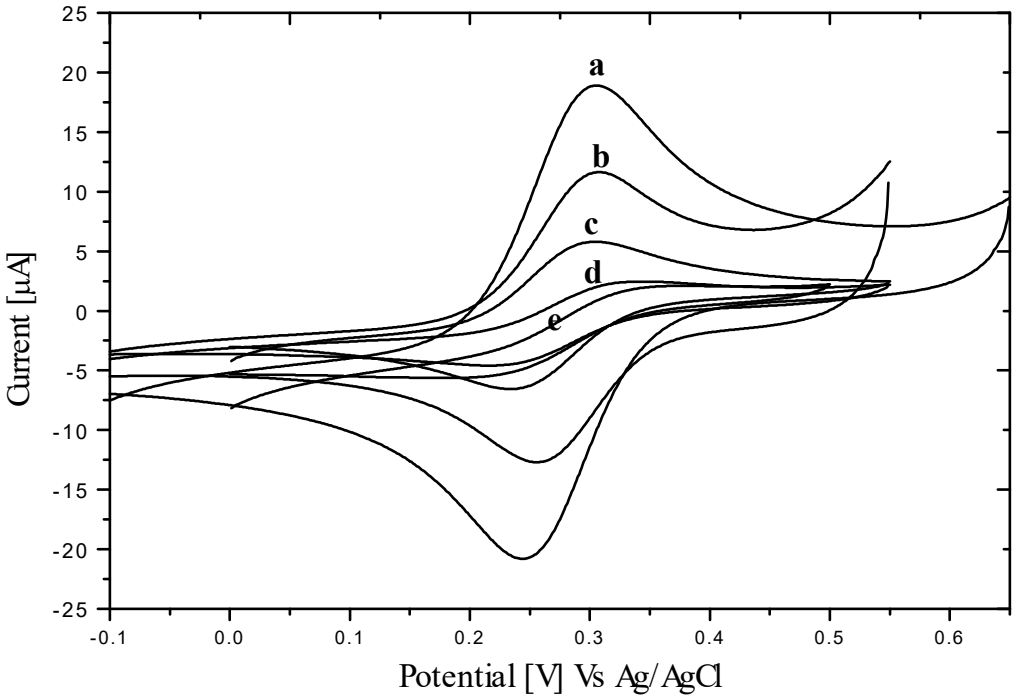


Figure 22. Cyclic voltammograms of 2 mM $K_3Fe(CN)_6$ in 1 M $KNO_3$ at Pt electrode modified with a) poly(3MT-co-3OT) b) P3MT, c) bare Pt d) poly(3HT-co-3OT) and e) P3OT at a scan rate of 20 mV/s .

$$Fe(CN)_6^{3-} + e^- \rightleftharpoons Fe(CN)_6^{4-} \qquad (1)$$

As can be seen from Figure 22 only P3MT and poly(3MT-co-3OT) catalyze the potassium ferricyanide redox system. A higher catalytic effect for poly(3MT-co-3OT) with a reduction

current of 20.43 µA was obtained as compaired to P3MT with a reduction current of 10.6 µA. Studies on the electrocatalytic behaviour of P3MT modified electrodes have been reported in the literature [52,58]. However as can be seen from Figure 22 the copolymer of 3MT and 3OT catalyze better than the pure P3MT.

Once the best polymer for electocatalysis was known, determination of the polymer thickness that catalyzes best was examined by varying the deposition time between 4 s and 14 s.

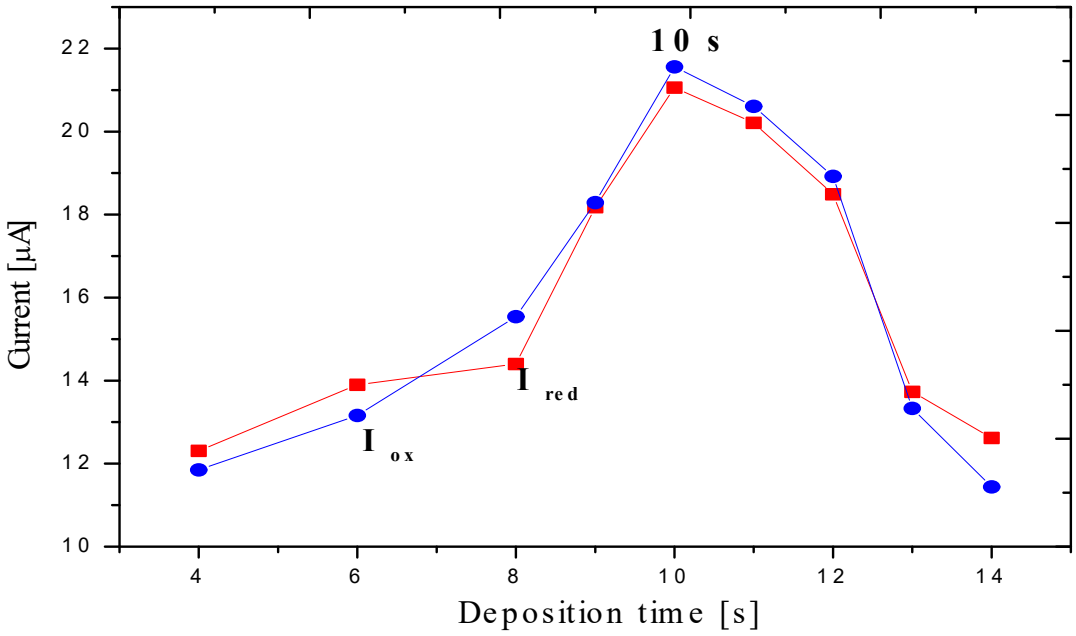


Figure 23. The effect of deposition time of poly(3MT-co-3OT) at a Pt electrode on the electrocatalytic activity of the redox system of 2 mM $K_3Fe(CN)_6$ in 1 M $KNO_3$ solution, at a polymerization potential of 2.00 V

Figure 23 shows that the electrocatalytic activity of poly(3MT-co-3OT) modified Pt electrodes depends on the film thickness. As the thickness increases the film becomes resistive and the current response decreases. On the other hand at low film thickness low catalytic effect was noticed. Therefore the optimum thickness was achieved at a deposition time of 10 s and further studies on poly(3MT-co-3OT) modified Pt electrode were done at this deposition time.

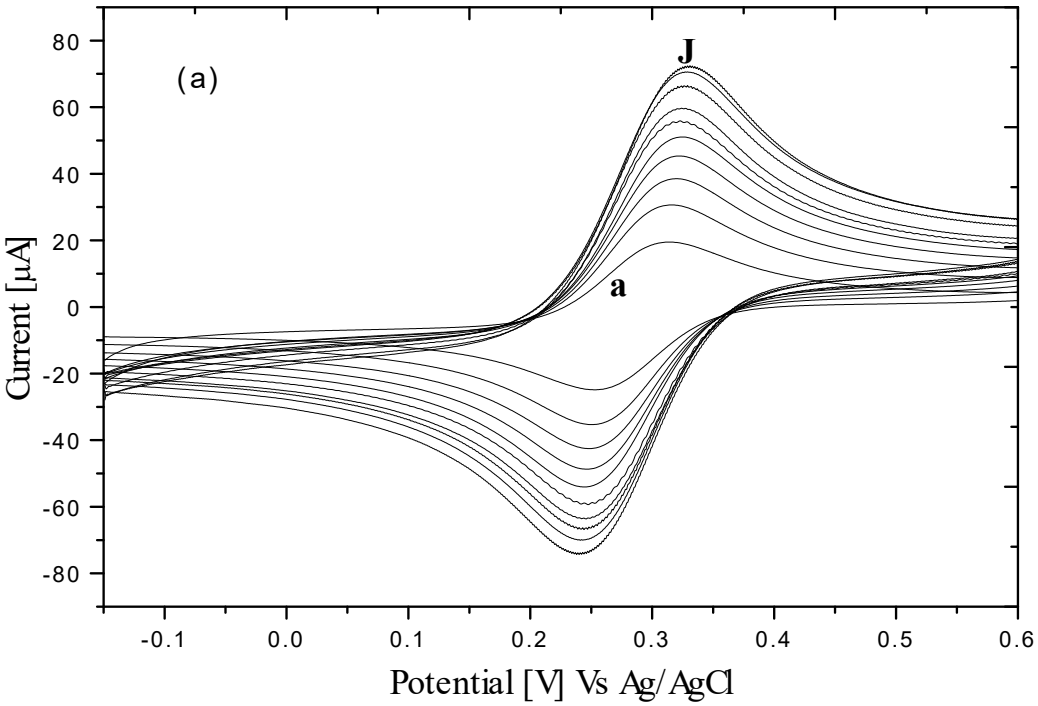


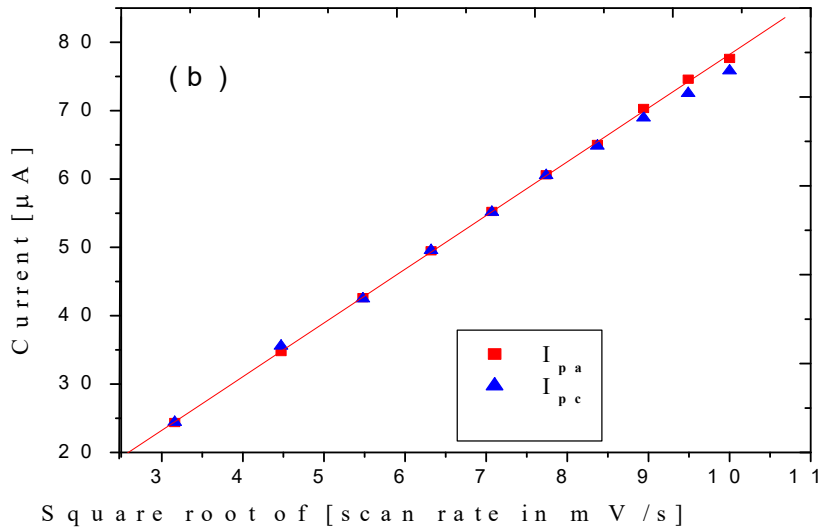


Figure 24. a) Cyclic voltammograms of 2 mM $K_3Fe(CN)_6$ in 1 M $KNO_3$ solution at a poly(3MT-co-3OT) modified Pt electrode, a)10 mV/s and j)100 mV/s with 10 mV/s interval.
b) Peak current *versus* square root of scan rate from the cyclic voltammogram in (a)

In order to examine the effect of repetitive cycles on the redox behavior the reaction was carried with repeated scans on the modified Pt electrode. After 10 scans it was noticed that the current response remains unchanged indicating that no adsorption of the redox species on the electrode. This indicates the stability poly(3MT-co-3OT) modified Pt electrode.

As can be seen from Figure 24 the redox peak currents are linearly proportional to the square root of the scan rates therefore, the mass transport in the redox process was diffusion controlled. So the peak current ( i*p* ) is consistent with the Randles Sevcik equation ($ip = 2.69 \times 10^5 n^{3/2} A D_O^{1/2} v^{1/2} C_O$ , for a diffusion controlled redox system, where; A is the electrode area ($cm^2$ ), n is the number of electrons transferred, $C_O$ is the concentration (mol $cm^{-3}$ ) and *v* is the scan rate in V/s). The reduction peak potential was obtained at 245 mV and the oxidation peak potential was obtained at 303 mV, with a peak separation, ΔEp, of 58 mV at poly(3MT-co-3OT) modified Pt electrode at a scan rate of 20 mV/s. The magnitudes of the reduction and the oxidation currents were 20.4 μ A and 20.5 μ A, respectively which is consistent with what obtained in Figure 24. The behavior observed was in agreement with the literature value for a reversible system with a one electron transfer [59].

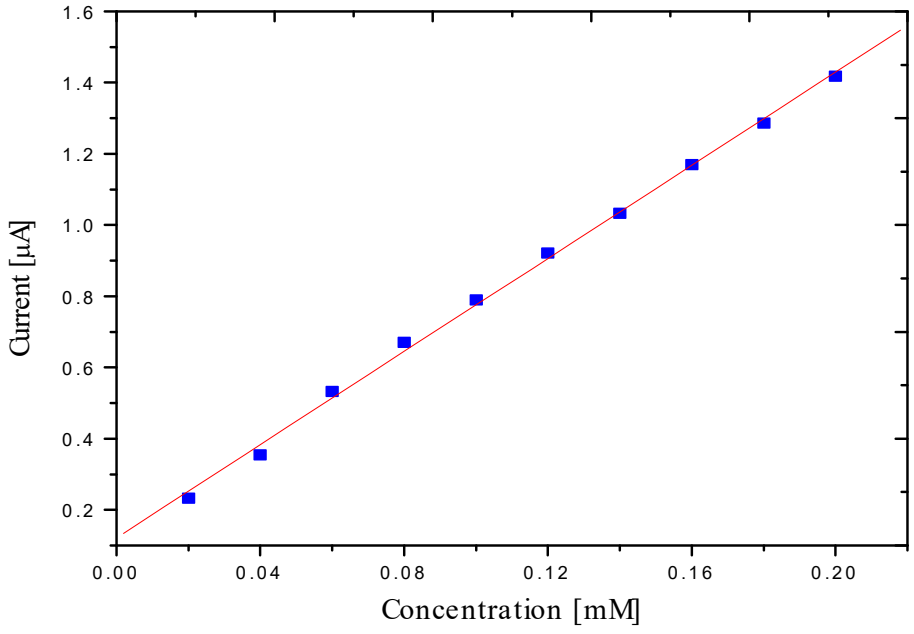


Figure 25. Effect of concentration of $K_3Fe(CN)_6$ on its reduction peak current at poly(3MT-co-3OT) modified Pt electrode, at a scan rate of 20 mV/s.

To examine the detection limit of the modified electrode studies were made by varying the concentration of potassium ferricyanide and measuring the reduction peak current. A lower detection limit of 20 µM of potassium ferricyanide was obtained. From the calibration curve the variation of the reduction peak current with varying concentration showed a linear dependance in the concentration range between 0.02 mM to 0.20 mM as shown in Figure 25.

Results obtained for the ferricyanide system were extended for other biological and environmental samples as presented in the following sections.

### 4.2.2 Electrochemical Behaviors of Catechol and Hydroquinone at a Poly(3MT-Co-3OT) Modified Pt Electrode

For both hydroquinone and catechol the working solution were prepared by appropriate dilution of the corresponding stock solutions with 0.1 M phosphate buffer and phosphoric acid in order to obtain the appropriate pH for a maximum response. The pH was varied from pH = 0 to pH = 10 using 1 M phosphoric acid, 0.1 M phosphate buffers and 0.1 M sodium hydroxide solutions.

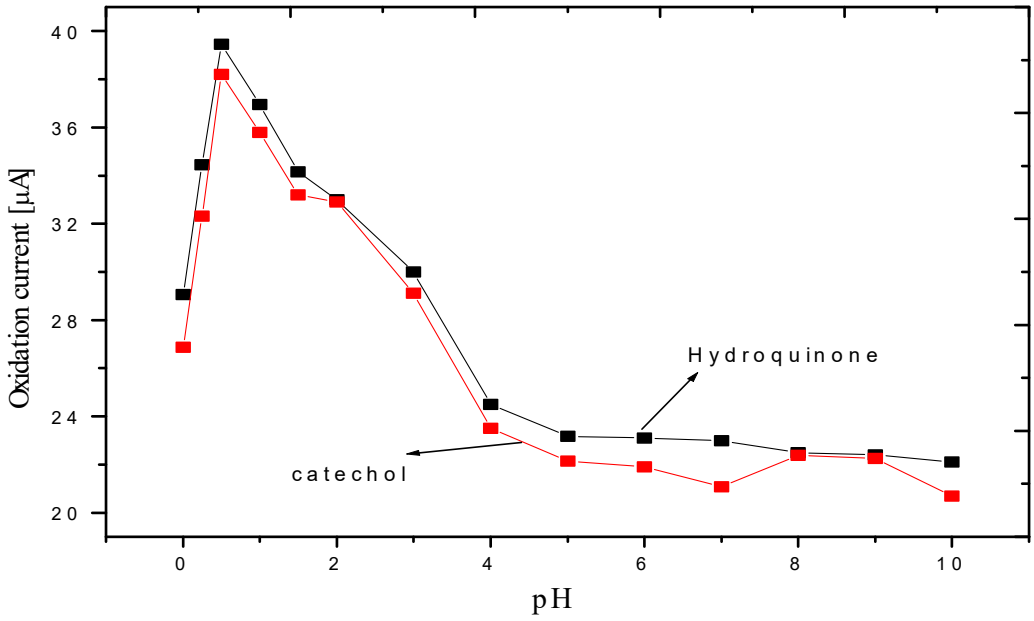


Figure 26. The oxidation peak current response *versus* solution pH from the cyclic voltammograms of 2 mM catechol and 2 mM hydroquinone at a poly(3MT-co-3OT) modified platinum electrode.

The current response for both cathecol and hydroquinone at different pH was determined and the maximum current response was obtained at pH 0.5 for both catechol and hydroquinone **(**Fig. 26). At higher pH the oxidation potentials of both analytes shifts towards a negative direction and a decrease in the redox current was observed. When the pH decreased a potential shift to a positive direction and an increase in the redox current is observed until the pH is 0.5. Below this pH value the current response starts to decrease.

Once the optimum pH was determined the electocatalytic behavior of the copolymer on the redox system of these analytes were studied at 0.3 M phosphoric acid solutions (pH = 0.5), which was prepared from phosphoric acid solution. Cyclic voltammograms (CV) of 2 mM hydroquinone at a scan rate of 20 mV/s in phosphoric acid solution (pH = 0.5) at poly(3MT-co-3OT) modified Pt electrode and at bare Pt electrodes are shown in Figure 27. At bare Pt electrode, the anodic peak and the cathodic peak of hydroquinone appeared at 658 mV and 224 mV, respectively, with the separation between oxidation peak and reduction peak potentials ($\Delta E_p$) of 434 mV. The large $\Delta E_p$ indicates that hydroquinone exhibits an irreversible electrochemical behavior at bare Pt electrode at that condition.

The oxidation peak current of hydroquinone at poly(3MT-co3-OT) modified Pt electrode greatly increased, compared with that at bare Pt electrode (Fig.27a), and the anodic peak and the cathodic peak appeared at 487 mV and 439 mV, respectively, with a peak separation ($\Delta E_p$) of 48 mV. The anodic peak potential shifted negatively from 658 mV to 487 mV and the cathodic peak potential shifted positively from 224 mV to 439 mV. This small $\Delta E_p$ indicates that the oxidation and reduction potentials of hydroquinone at poly(3MT-co-3OT) modified Pt electrode are becoming closer and the electrochemical reversibility of hydroquinone at the modified Pt electrode is much improved.

The $\Delta E_p$ of 48 mV was consistent with the literature value of 46 mV at which hydroquinone undergoes oxidation to the corresponding benzoquinone by a transfer of two electrons and two protons in acidic media [50, 60] as shown in Equation 2. The stability of poly(3MT-co-3OT) modified electrode towards detection of hydroquinone was examined by scanning for ten repetitive cycles (Fig. 27a), where no change in the current response was observed.

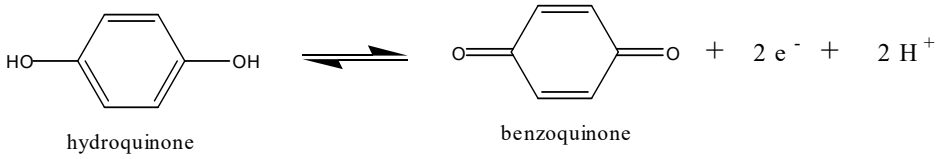


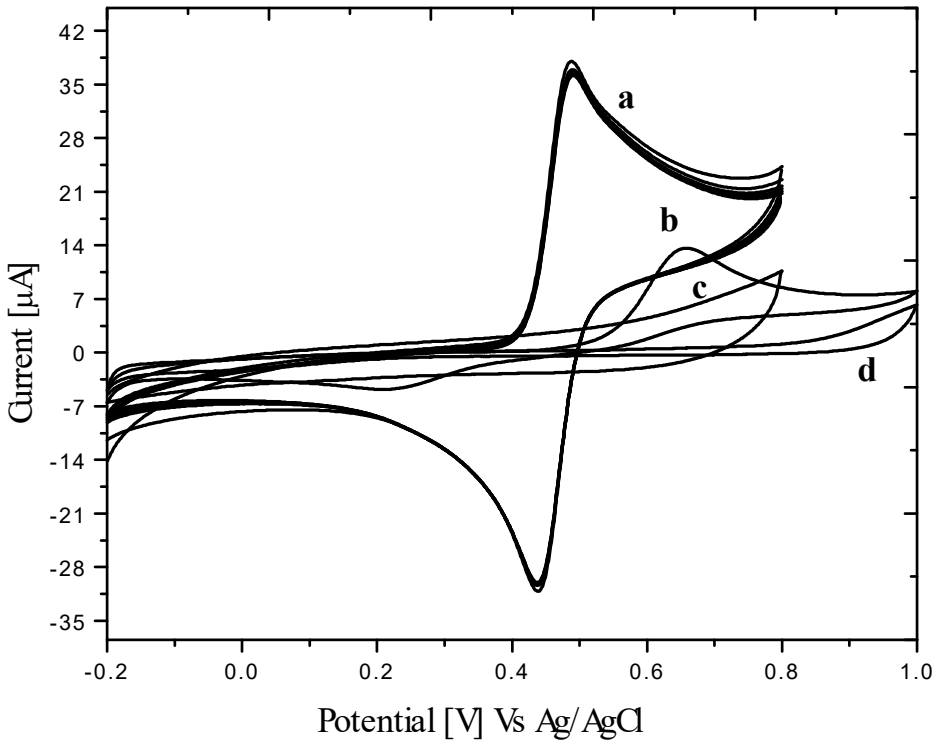


Figure 27. Cyclic voltammogram of 2 mM hydroquinone a) at poly(3MT-co-3OT) modified Pt electrode b) at bare Pt electrode c) and d) are cyclic voltammograms of the supporting electrolyte on modified and bare Pt electrode respectively at pH = 0.5 phosphoric acid solution, at a scan rate of 20 mV/s.

The cyclic voltammogram of 2 mM catechol at a Pt electrode modified with poly(3MT-co-3OT) is also compared with that of bare Pt electrode at a scan rate of 20 mV/s in 0.3 M phosphoric acid solution (pH 0.5) (Fig. 28). At a bare Pt electrode, the anodic peak potential and the cathodic peak potential of catechol were 709 mV and 411 mV, respectively, with $\Delta E_p$ of catechol being 298 mV. At poly(3MT-co-3OT) modified Pt electrode, the oxidation peak current of catechol greatly increased and the anodic peak and the cathodic peak potentials appeared at 596 mV and 539 mV, respectively, with $\Delta E_p$ of catechol at poly(3MT-co-3OT) Pt electrode being 57 mV. This result indicates that the oxidation peak current of catechol at the

poly(3MT-co-3OT) modified Pt electrode is significantly enhanced and the oxidation potential of catechol at poly(3MT-co-3OT) modified Pt is much lowered. The $\Delta E_p$ value of 57 mV obtained was consistent with the literature value of 57 mV at which catechol undergo oxidation to the corresponding o-quinone by a transfer of two electrons and two protons in acidic media [50, 60, 61] as shown in Equation 3. Similar stability behavior of the poly(3MT-co-3OT) modified Pt electrode like that of hydroquinone was observed with ten repetitive cycles as shown Figure 28a.

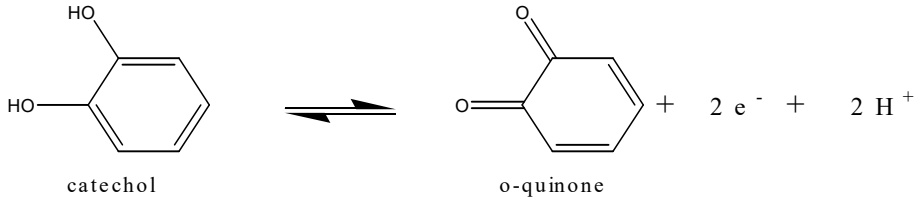


(3)

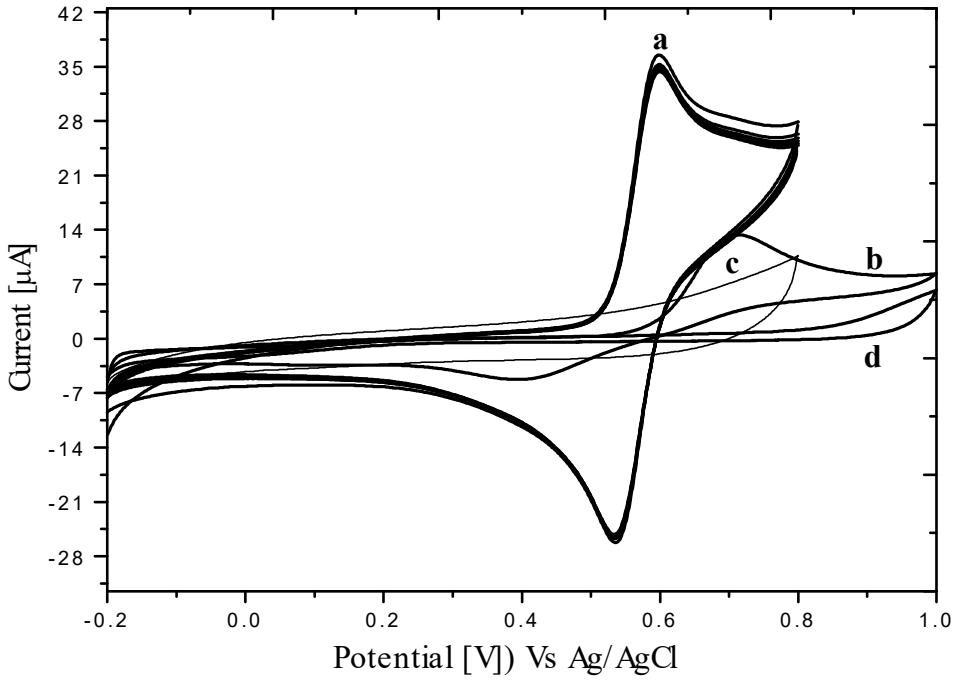


Figure 28. Cyclic voltammogram of 2 mM catechol a) at poly(3MT-co-3OT) modified Pt electrode b) at bare Pt electrode c) and d) are cyclic voltammograms of the supporting electrolyte on modified and bare Pt electrodes respectively at pH = 0.5 phosphoric acid solution, at a scan rate of 20 mV/s.

### 4.2.3 The Simultaneous Determination of Catechol and Hydroquinone

In ranges above pH = 1.5 the oxidation peaks of both catechol and hydroquinone are observed as a single broad peak with no separation. Below pH = 1.5 the oxidation peaks started to be separated and at pH = 0.5 the maximum separation as well as maximum current were observed. Below this pH even though the peaks are still separated the oxidation current was decreased. Therefore the optimum pH for the detection of both catechol and hydroquinone was obtained to be the same whether they are detected simultaneously or in the absence of the other.

The reduction potential peaks of catechol and hydroquinone are separated in a wide pH range while the oxidation potential peaks do not separate, therefore the oxidation peak potential and currents were taken as a parameter for the simultaneous detection of these two analytes. The cyclic voltammogram of equimolar mixture of catechol and of hydroquinone at bare Pt electrode and at poly(3MT-co-3OT) modified Pt electrode at a scan rate of 20 mV/s in 0.3 M phosphoric acid solution (pH 0.5) showed that the oxidation peak of hydroquinone and the oxidation peak of catechol merged into a broad peak at 727 mV at bare Pt electrode (Fig. 29b)

Hydroquinone and catechol at poly(3MT-co-3OT) modified Pt electrode yielded two well-defined oxidation peaks, at potentials of 494 mV and 598 mV, respectively with 104 mV separation between the corresponding anodic peaks of hydroquinone and catechol (Fig. 29a). The oxidation peak currents also increased remarkably at poly(3MT-co-3OT) modified Pt electrode. The modified electrode was stable for simultaneous detection of hydroquinone and catechol for ten repetitive cycles as shown in Figure 29a. In addition to this using poly(3MT-co-3OT) modified Pt electrode, there was no shift in redox potentials of catechol and hydroquinone whether they are detected alone or in the presence of the other (simultaneously) (Fig. 30). So this shows that poly(3MT-co-3OT) modified Pt electrode is highly sensitive and selective for simultaneous detection of catechol and hydroquinone. The increase in anodic current responses and the lowering in separation peak potential ($\Delta E_p$ ) of both Hydroquinone and catechol arise from electrochemical modification of Pt electrode with poly(3MT-co-3OT).

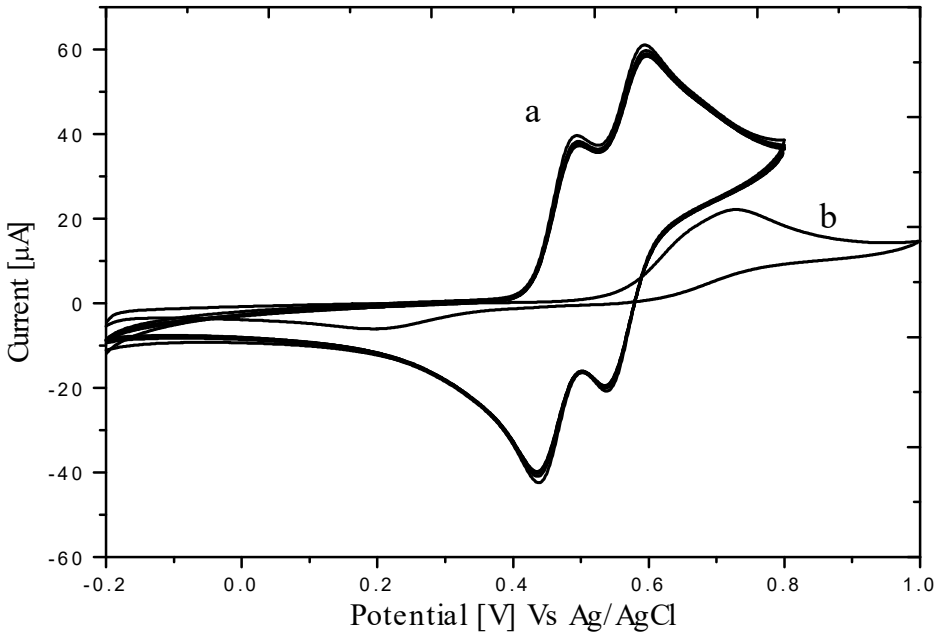


Figure 29. Cyclic voltammograms of equimolar (2 mM) mixtures of cathecol and Hydroquinone at a) poly(3MT-co-3OT) modified Pt electrode and b) bare Pt electrode in 0.30 M phospheric acid pH = 0.5 solution.

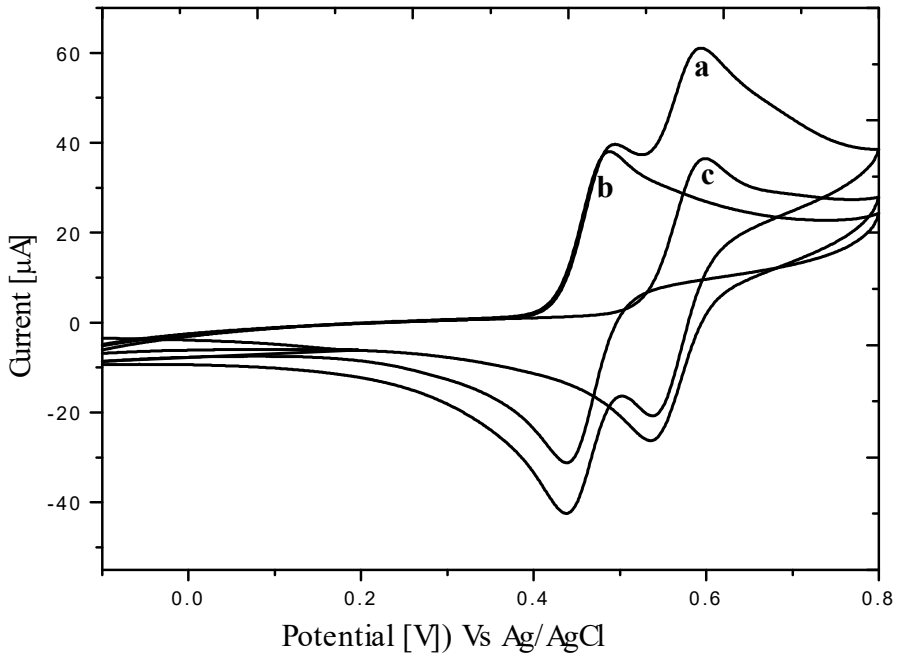


Figure 30. Cyclic voltammograms of cathecol and hydroquinone a) equimolar (2 mM) mixtures b) hydroquinone (2 mM) alone, c) catechol (2 mM) alone at poly(3MT-co-3OT) modified Pt electrode in 0.3 M phosphoric acid pH = 0.5.

To study the electrochemical behaviour of the system in the simultaneous determination of catechol and hydroquinone, the effect of scan rate on the oxidation peak currents and peak potentials of both catechol and hydroquinone were examined using cyclic voltammetry at poly(3MT-co-3OT) modified platinum electrode in a solution containing equimolar concentrations (2 mM) of both analytes (Fig. 31).

It was found that the change in redox peak potentials of both catechol and hydroquinone and the separation between the redox peak potentials of the two were insignificant with varying the scan rate from 20 mV/s to 200 mV/s, which suggests that the redox processes of catechol and hydroquinone are diffusion controlled. It was also found that the oxidation peak currents of both catechol and hydroquinone were directly proportional to the square root of the scan rate between 20 mV/s and 200 mV/s as shown in Figure 32. This is consistent with Randles Sevcik equation indicating that the electrochemical process is diffusion controlled.

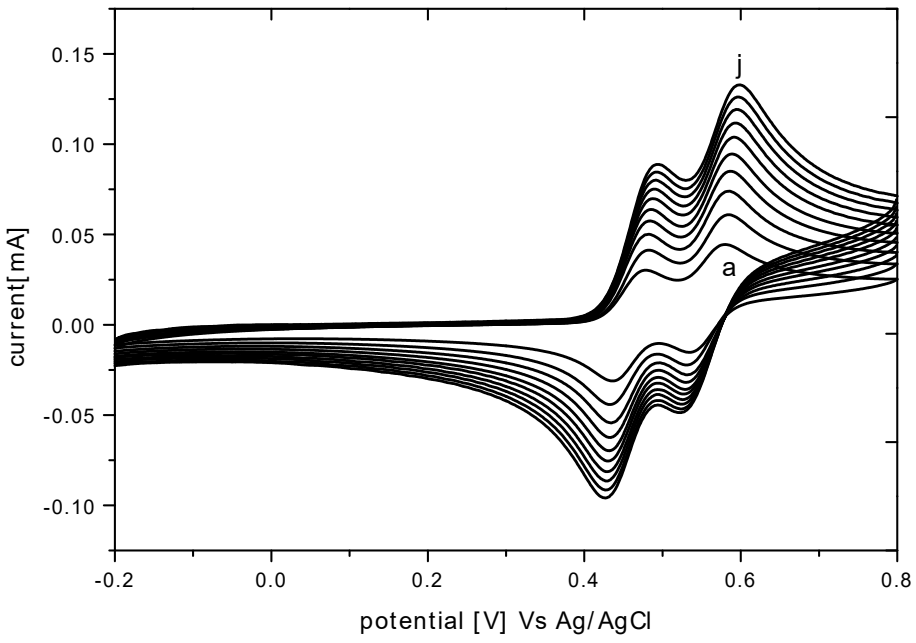


Figure 31. Cyclic voltammograms of equimolar (2 mM) mixtures of cathecol and hydroquinone at different scan rates, (a) 20 mV/s and (j) 200 mV/s with 20 mV/s interval.

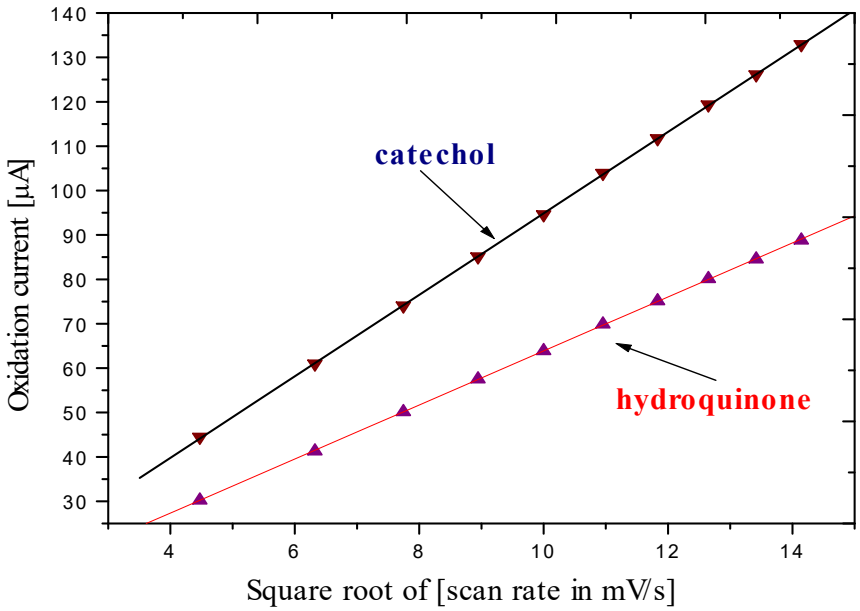


Figure 32.The effect of scan rate on the oxidation currents of equimolar (2 mM) mixtures of catechol and hydroquinone at different scan rates.

Because of its excellent selectivity and sensitivity differential pulse voltammetry (DPV) was used in this work to see the detection of one analyte in the presence of high concentration of the other. In order to simultaneously determine hydroquinone and catechol, the calibration plot for hydroquinone in the presence of catechol and the calibration plot for catechol in the presence of hydroquinone were obtained by using of DPV at poly(3MT-co-3OT) modified Pt electrode with optimized condition (Fig. 33,35). The parameters used for DPV were a scan rate of 20 mV/s, pulse amplitude of 50 mV, pulse width of 50 ms and pulse period of 200 ms. Under these optimized conditions, the calibration plots for hydroquinone and catechol were obtained using DPV at poly(3MT-co-3OT) modified Pt electrode. The oxidation peak current of catechol increased with an increase in catechol concentration (Fig. 33). In the presence of 0.4 mM hydroquinone the oxidation peak current of catechol was linear in the range from 40 μM to 0.4 mM catechol concentration (Fig. 34).

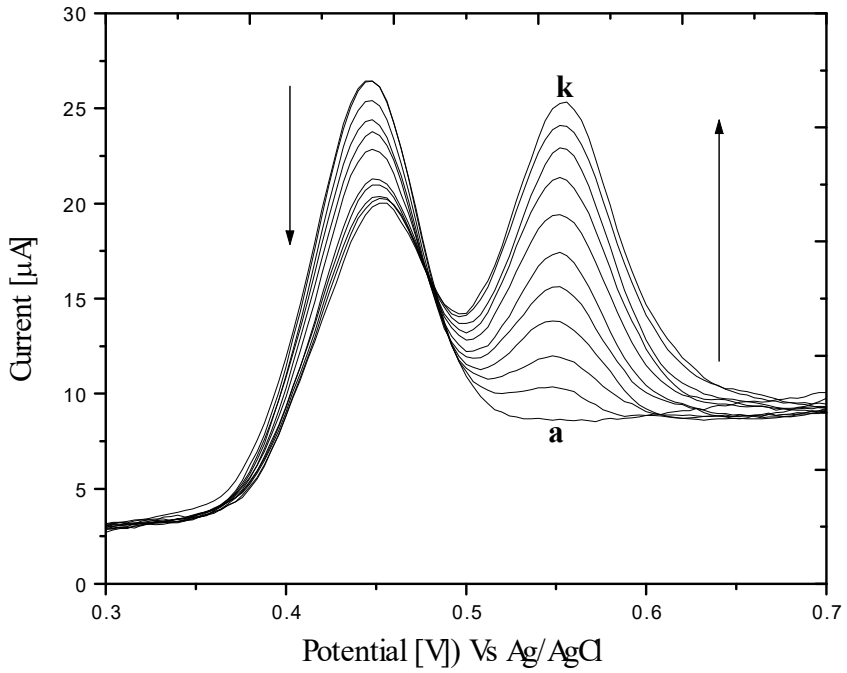


Figure 33. DPV of catechol at a) 0 M, b) 40 µM to k) 0.4 mM varying concentration in a solution containing 0.4 mM hydroquinone at poly(3MT-co-3OT) modified Pt electrode in pH = 0.5 phospheric acid solution.

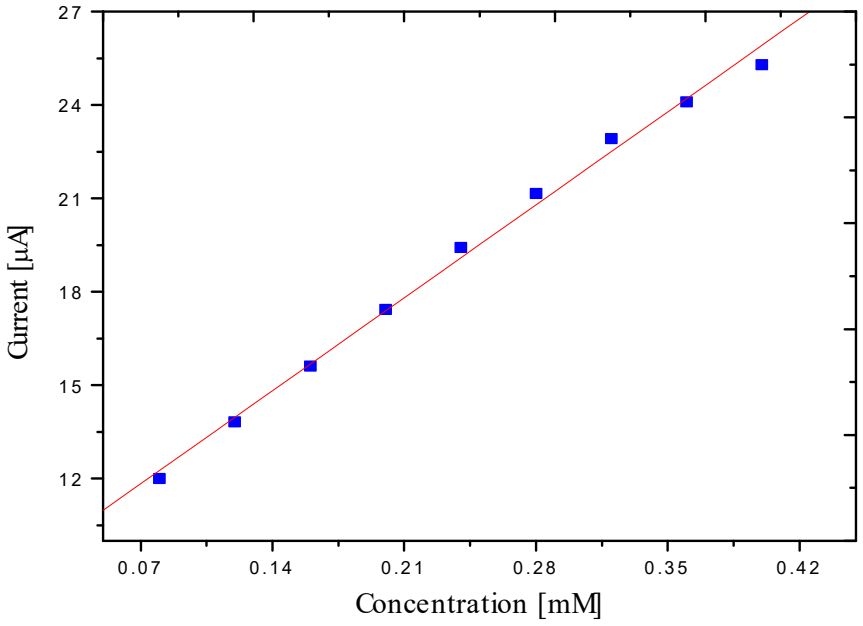


Figure 34. The calibration curve for catechol from the DPV in Figure 33 in the range of 40 µM to 0.4 mM.

Similarly the oxidation peak current of hydroquinone increased with increasing in hydroquinone concentration (Fig. 35). In the presence of 0.4 mM catechol the oxidation peak current of hydroquinone was linear in the range of 40 μ M to 0.4 mM hydroquinone concentration with (Fig. 36). From Figures 33 and 35 a decrease in the oxidation currents at constant concentrations of catechol as well as hydroquinone instead of being constant, might be due to the surface adsorption of the oxidized analytes, which covers the electrode surface. However, in case of the cyclic voltammetry of the same solution no decay of current was observed due to the presence of the reverse scan which reduces the analytes back (Fig. 29).

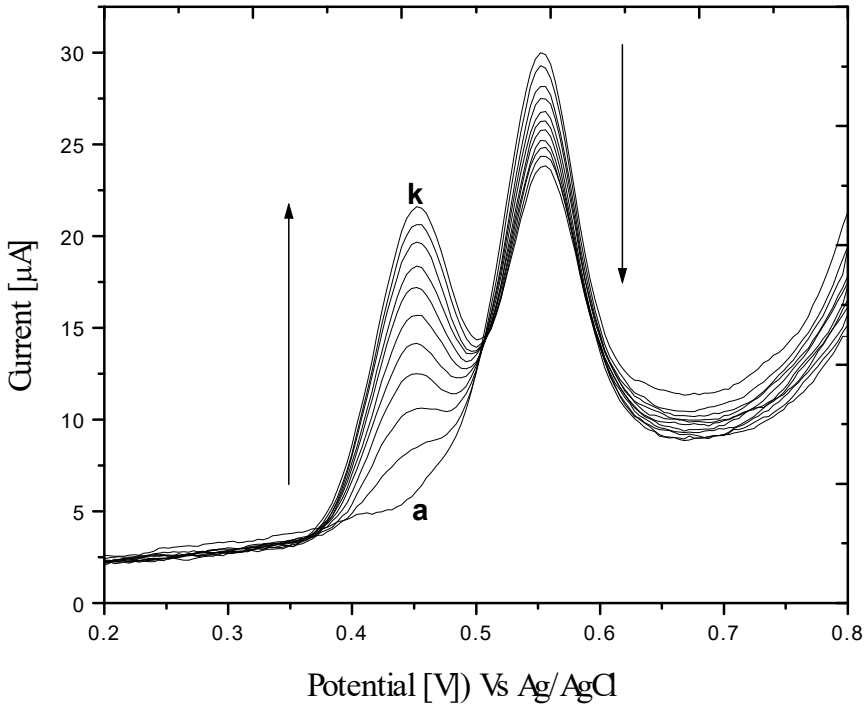


Figure 35. DPV of hydroquinone at a) 0 M, b) 40 μM to k) 0.4 mM varying concentration in a solution containing 0.4 mM catechol at poly(3MT-co-3OT) modified Pt electrode in pH = 0.5 phospheric acid solution.

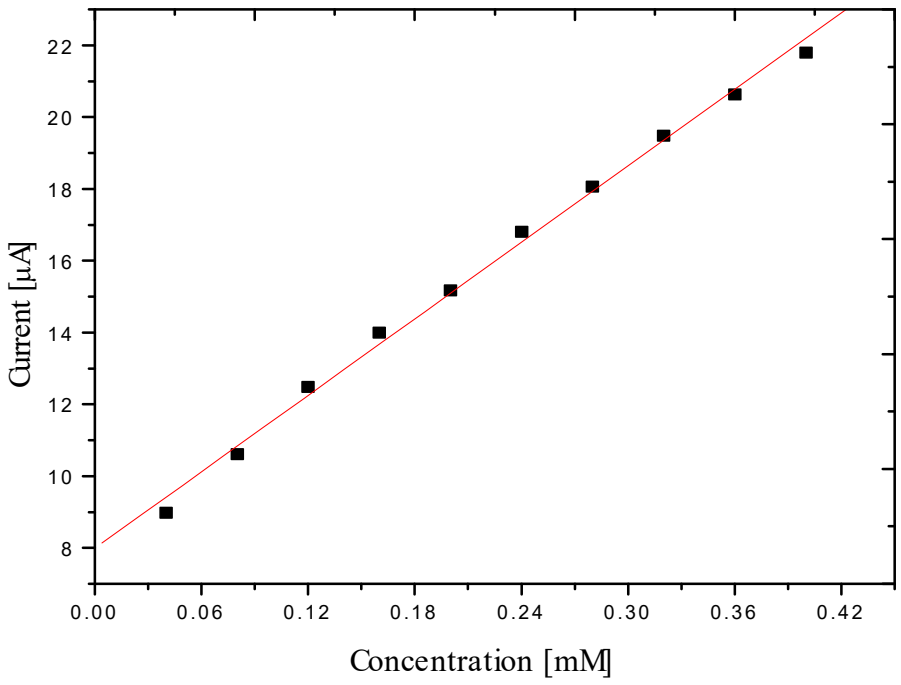


Figure 36. The calibration curve for hydroquinone from the DPV in Figure 35 in the range of 40 μM to 0.4 mM.

### 4.2.4 Electrochemical Behaviors of Ascorbic Acid

Solution of ascorbic acid were prepared by appropriate dilution of 0.1 M ascorbic acid with 0.1 M phosphate buffer and phosphoric acid for lower pH solutions and 0.1 M sodium hydroxide for higher pH solutions. Optimum condition for maximum oxidation current response of ascorbic acid was determined at different pH between pH = 1 and 10. The maximum current response was obtained at pH 4.0 (Fig. 37). During the variation of the pH of the solution, a positive shift in oxidation potential was observed at lower pH and a negative shift in oxidation potential was observed at higher pH values. The higher oxidation current response at a pH of around 4.0 was consistent with the literature report for N,N-dimethylaniline modified glassy carbon electrode [54]. The acid will be in an anionic form at around pH = 4.0 and the maximium oxidation current response might be due to the electrostatic attraction of the anionic ascorbic acid with a positively charged polymer, which facilitate its adsorption on the electrode.

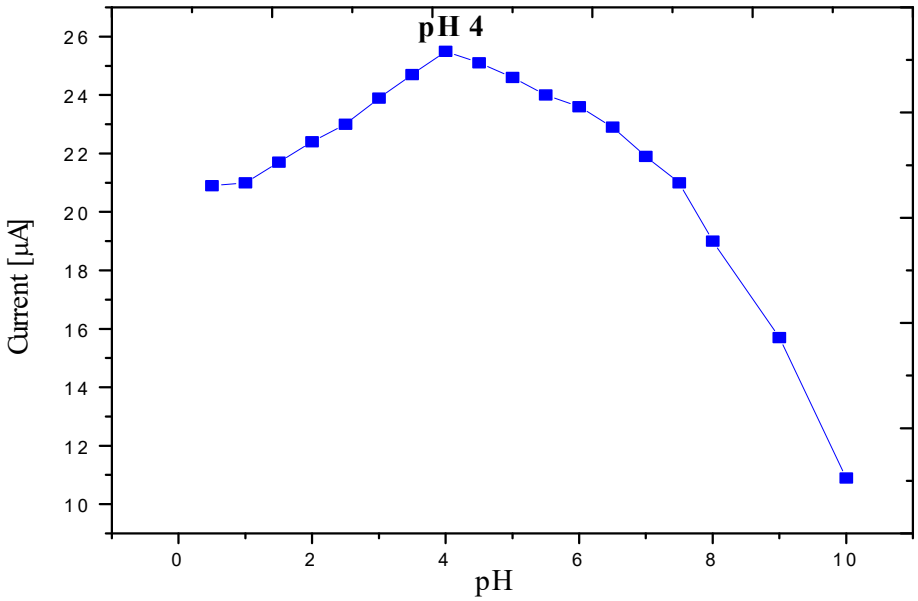


Figure 37. Effect of pH on oxidation peak current of 2 mM ascorbic acid at poly(3MT-co-3OT ) modified Pt electrode.

As the pH of the solution increases the current response decreases. At pH values around 4.0 ascorbic acid is oxidized to the corresponding dehydroascorbic acid, with a transfer of two electrons and two protons as shown in Equation 4 [54]. Once the optimum pH was determined the oxidation of ascorbic acid (AA) was examined on both electrodes (bare Pt electrode and poly(3MT-co-3OT) modified Pt electrode).the result obtained was as shown in Figure 38.

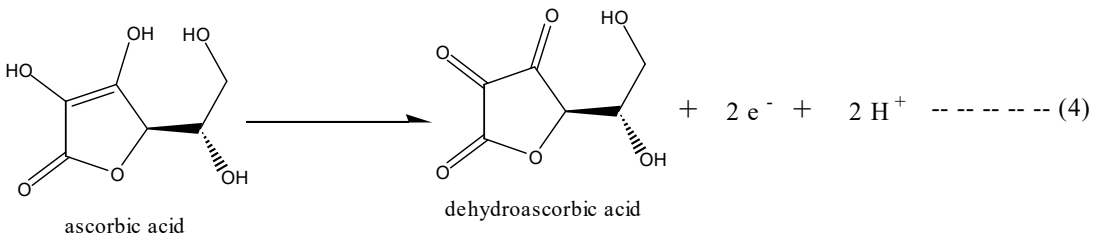

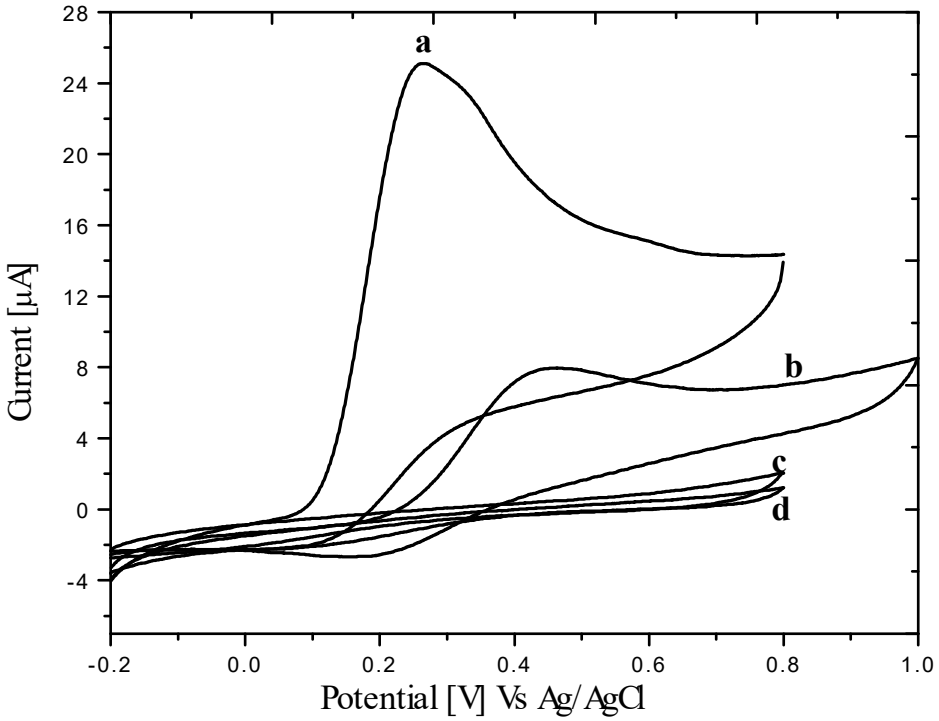


Figure 38. Cyclic voltammogram of 2 mM ascorbic acid in pH = 4.0 phosphate buffer a) at a poly(3MT-co-3OT) modified Pt electrode first cycle b) at bare Pt electrode first cycle c) and d) are cyclic voltammograms of the supporting electrolyte at poly(3MT-co-3OT) modified Pt and bare Pt electrode, respectively, at a scan rate of 20 mV/s

From Figure 38 poly(3MT-co-3OT) has a good electrocatalyic effect of ascorbic acid as shown by increase in the oxidation peak current. Modification also shifts the oxidation potential of ascorbic acid towards negative potentials as compared to the bare Pt electrode.

Bare Pt electrode is unsuitable to monitor AA oxidation efficiently because oxidation of AA at a bare Pt electrode is associated with fouling of the electrode surface due to the oxidized product of ascorbic acid. As a result the electrochemical response consists of an ill-defined anodic peak, decreasing in height by repetitive cycling of the electrode potential (Fig 39d, e). This behavior supports the need to find an alternative electrode system for monitoring AA. The effective electrocatalytic activity of poly(3MT-co-3OT) towards AA oxidation is shown by the curves depicted in Figure 39a, b, c, where the cyclic voltammograms of the modified

electrode in phosphate buffer solution (pH = 4.0), are compared with the bare electrode (Fig. 39d, e).

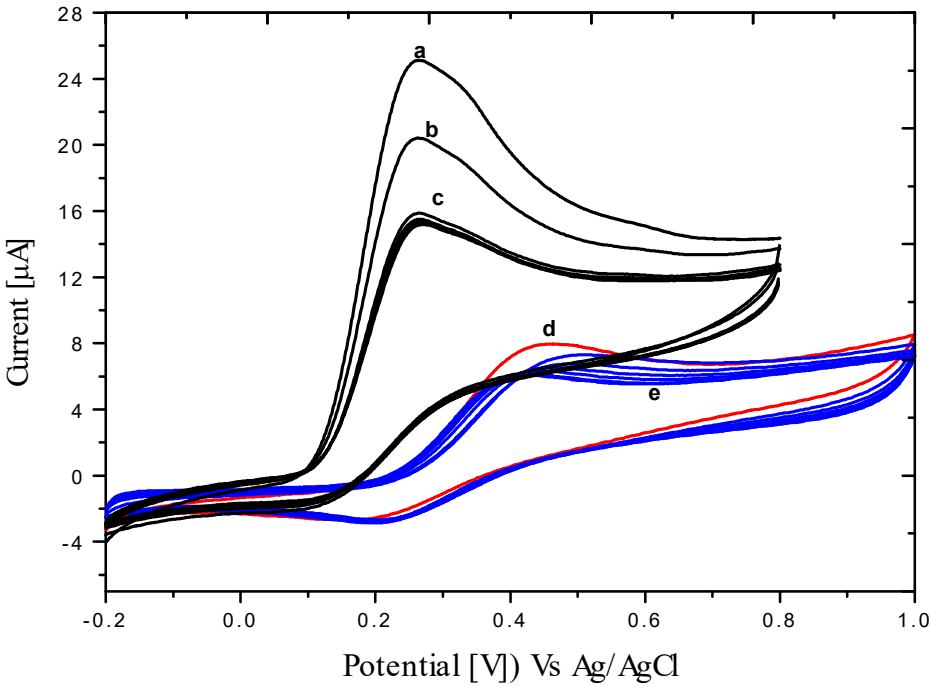


Figure 39. Cyclic voltammogram of 2 mM ascorbic acid at poly(3MT-co-3OT) modified Pt electrode a) first cycle, b) second cycle, c) last ten cycles, and at bare Pt electrode d) first cycle, e) last ten cycles in pH = 4.0 phosphate buffer.

From Figure 39c it can be seen that the first voltammogram recorded using poly(3MT-co-3OT) modified Pt electrode was different from the subsequent scans. With subsequent scans, the current slowly decreases reaching a stable value after two cycles. The stability was checked by series of 10 consecutive scans and no significant changes of the response were noticed. These results support the possibility of performing efficient analyses for long periods of time, using the modified electrode in calibration analysis at different AA concentrations. Calibration analysis at different AA concentrations was also performed in order to test the actual capabilities of this system using differential pulse voltammetry. The parameters used were a scan rate of 20 mV/s, pulse amplitude of 50 mV, pulse width of 50 ms and pulse period of 200ms.

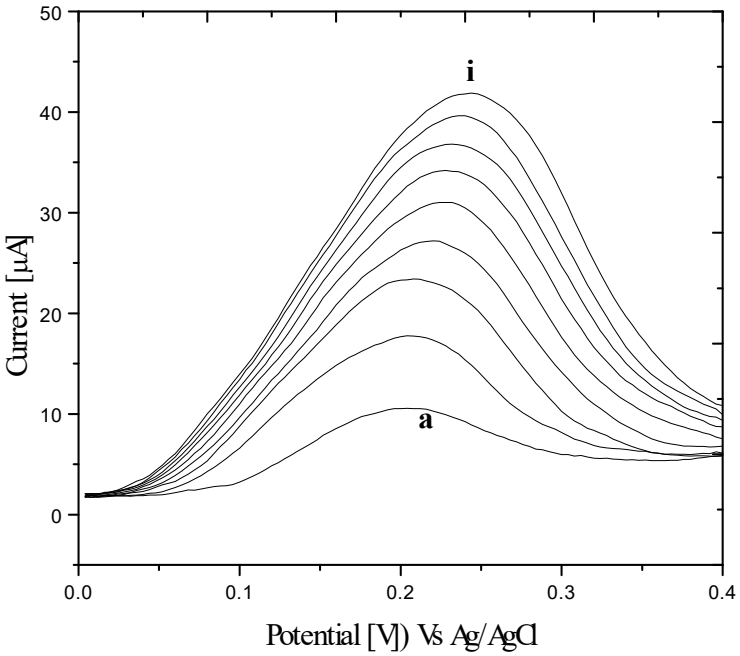


Figure 40. DPV of ascorbic acid at various concentration of ascorbic acid from a) 80 µM to i) 0.4 mM.

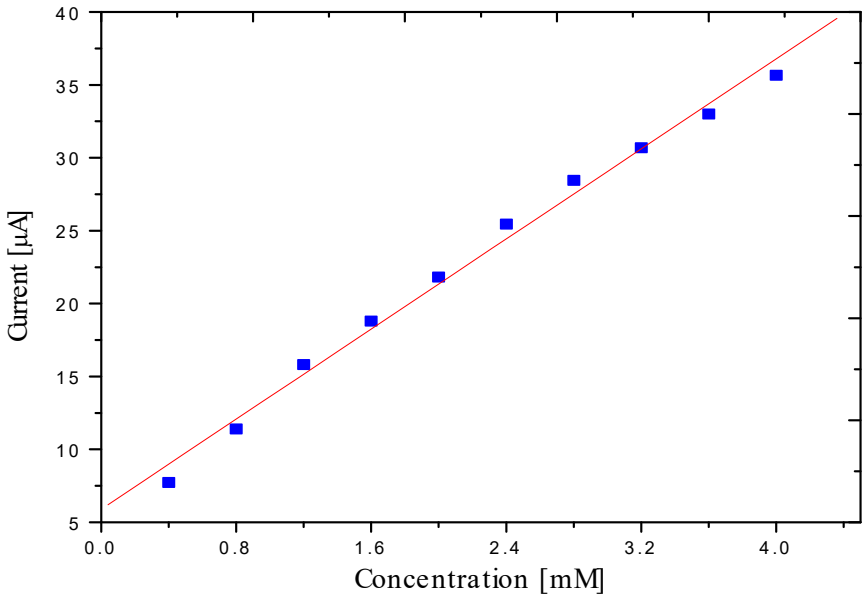


Figure 41. The calibration curve for ascorbic acid from the DPV in figure 40 in the range of 80 µM to 0.4 mM.

As can be depicted in Figure 40 an increase in oxidation current of ascorbic acid was observed with an increase in concentration of ascorbic acid. The calibration curve shows a linear dependence of the oxidation peak current on ascorbic acid concentration, from 80 µM to 0.4 mM (Fig. 41).

### 4.2.5 The Simultaneous Determination of Ascorbic Acid and Catechol

When the cyclic voltammogram of equimolar amount of ascorbic acid and catechol were recorded at a bare platinum electrode with the same condition where ascorbic acid was studied the oxidation peaks of the two analytes did not appear with a clear separation. Using poly(3MT-co-3OT) modified platinum electrode at higher pH ranges both analytes appeared at the same potential with a broad peak; while at very low pH values even though the oxidation peak current of catechol was increased the oxidation peak of ascorbic acid was decreased. However at a pH of 4.0 the oxidation peak potentials of ascorbic acid and catechol were obtained at 250 mV and 492 mV with a peak separation of 242 mV between the

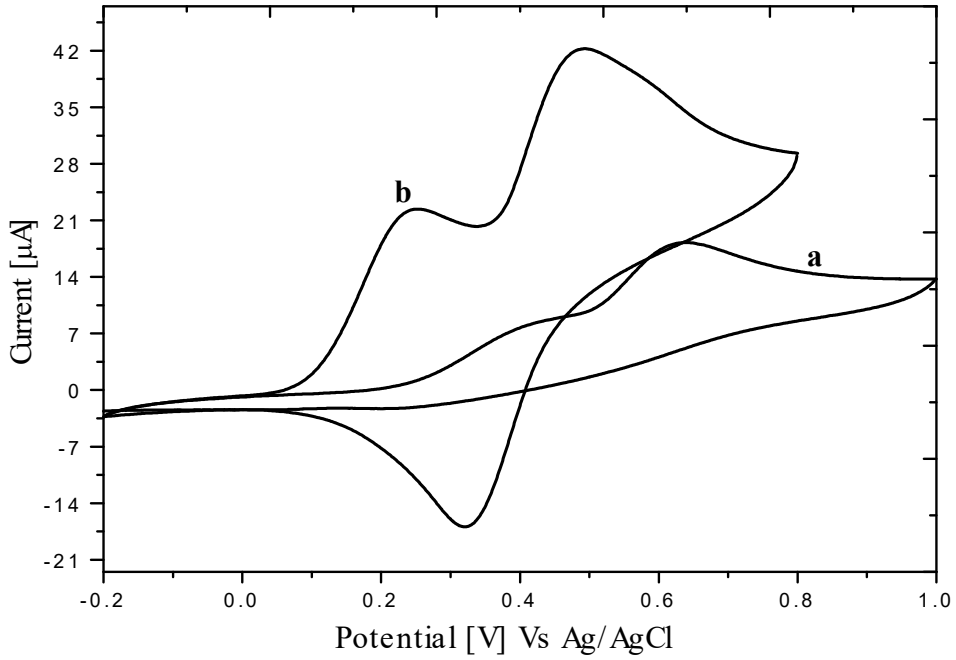


Figure 42. Cyclic voltammogram of equimolar mixture (2 mM) of ascorbic acid and catechol a) at bare platinum b) at poly(3MT-co-3OT) modified Pt electrode at pH = 4.0 phosphate buffer solution, at a scan rate of 20 mV/s.

oxidation peak potentials of the two (Fig. 42).The electrochemical behaviour of catechol at this pH was different from pH = 0.5 where it was detected together with hydroquinone. At pH = 4.0 its oxidation and reduction peak potentials were shifted negatively to 455 mV and 299 mV, respectively with large increase in $\Delta E_p$.

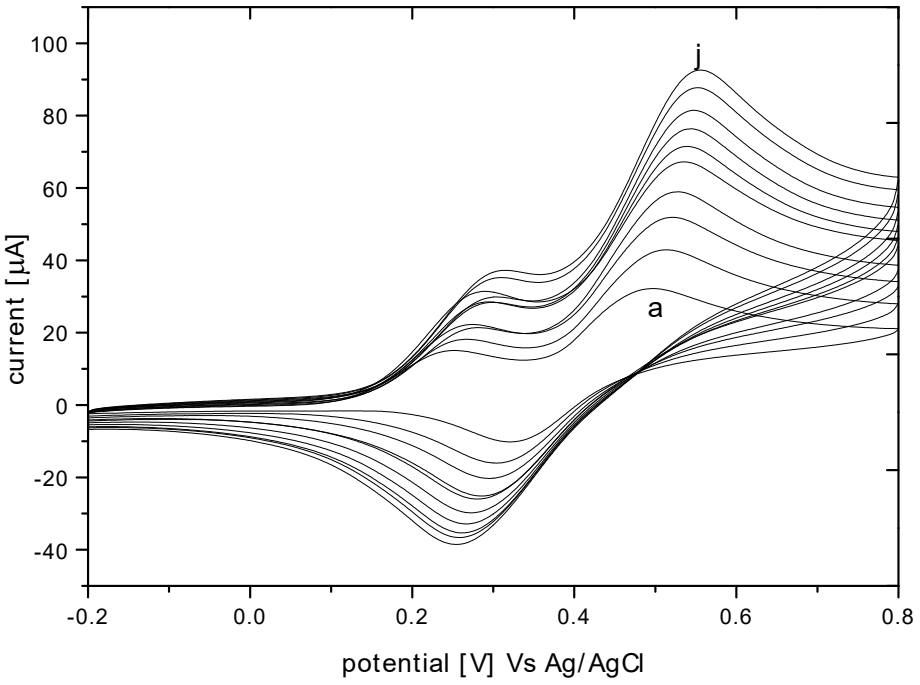


Figure 43. Cyclic voltammograms of equimolar (2 mM) mixtures of catechol and ascorbic acid at different scan rates, (a) 20 mV/s and (j) 200 mV/s with 20 mV/s interval.

The electrochemical studies on the simultaneous determination of catechol and ascorbic acid were done by examining the effect of scan rate on the oxidation peak currents and peak potentials of both catechol and ascorbic acid using cyclic voltammetry at poly(3MT-co-3OT) modified platinum electrode in a solution containing equimolar concentrations of both analytes (Fig. 43).

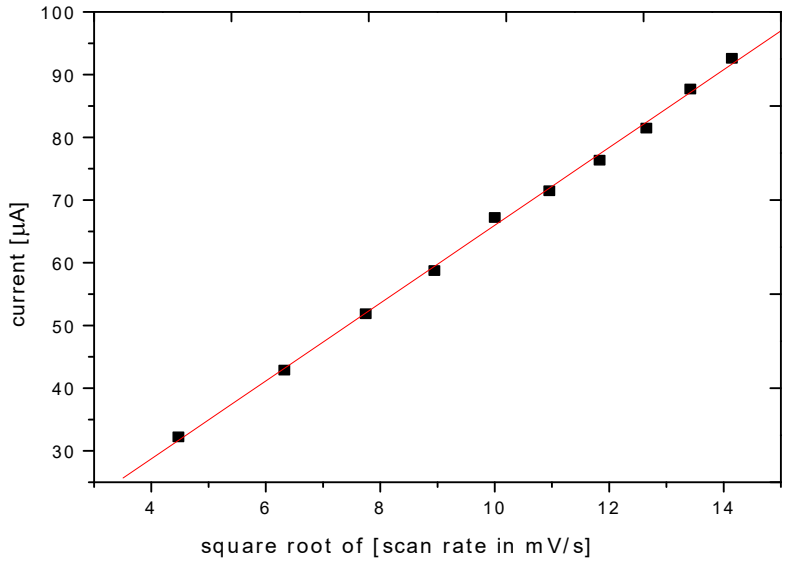


Figure 44. The effect of scan rate on the oxidation currents of catechol in equimolar (2 mM) mixtures of catechol and ascorbic acid at different scan rates.

It was found that the redox peak potentials of both catechol and ascorbic acid showed a small shift to a higher potential with scan rate from 20 mV/s to 200 mV/s which suggests that the redox processes of catechol and ascorbic acid are not fully diffusion controlled. Although a small shift in potential was observed the oxidation peak currents of catechol was directly proportional to the square root of the scan rate from 20 mV/s to 200 mV/s as shown in Figure 44, which is consistent with Randles Sevcik equation indicating that the mass transport is diffusion controlled. However, deviation from linearity of the oxidation current with square root of scan rate was observed for ascorbic acid. The deviation of ascorbic acid oxidation peak current with square root of scan rate was due to the complicated and stepwise electron transfer during the oxidation in which intermediates with varying adsorption and deadsorption extent are involved. Initially a one electron transfer leads to monodehydroascorbate radical, which is adsorbed, on the electrode surface, and it is further oxidized to adsorbed dehydroascorbic acid, afterwards dehydroascorbic acid undergoes a slow deadsorption [55].

For simultaneous determination of both ascorbic acid and catechol a DPV was used with a scan rate of 20 mV/s, pulse amplitude of 50 mV, pulse width of 50 ms and pulse period of 200

ms. In the presence of 40 μM ascorbic acid the DPV of of catechol at different concentration were obtained as shown in Figure 45. The oxidation peak current grows with concentration.

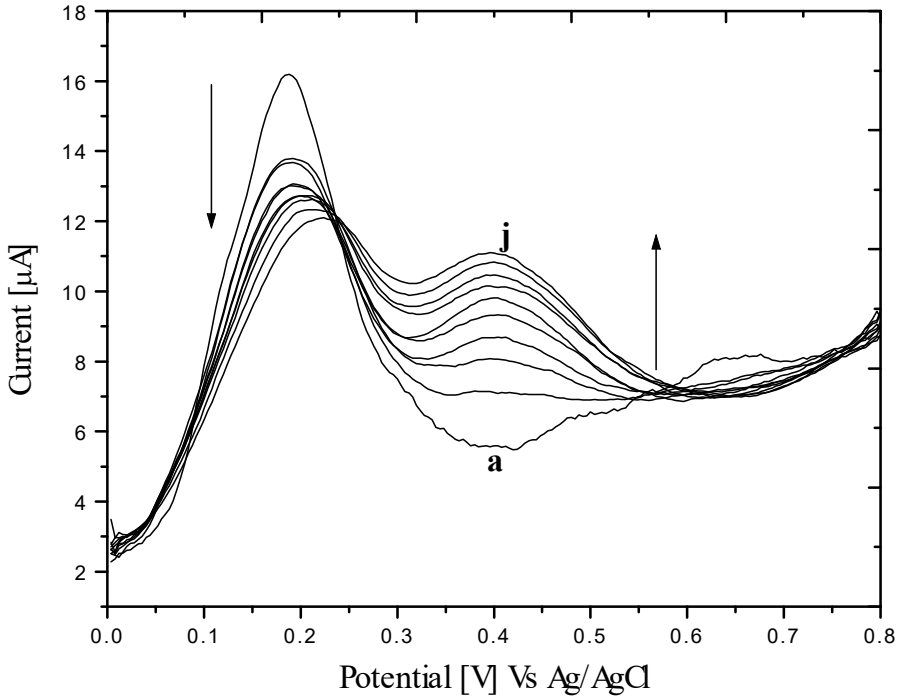


Figure 45. Differential pulse voltammogram of catechol at a) 0 M, b) 80 μM to j) 0.4 mM varying concentration in a solution containing 0.4 mM ascorbic acid at a poly(3MT-co-3OT) modified Pt electrode.

The calibration curve in Figure 46 shows a linear dependence of the oxidation peak current of catechol with its concentration, in the range from 80 μM to 0.4 mM. At fixed concentration of catechol and varying concentration of ascorbic acid the growth of DPV of ascorbic acid with concentration was not significant due to large peak width of ascorbic acid and the unstability of the first few cycles in the oxidation of ascorbic acid.

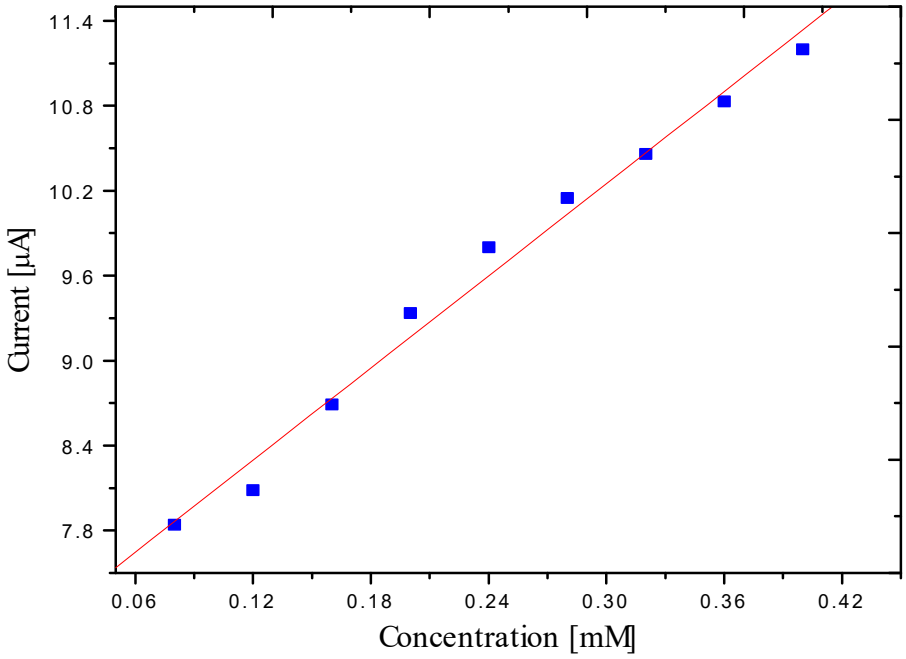


Figure 46. The calibration curve for catechol from the DPV in figure 45 in the range of 80 μM to 0.4 mM.

## 5. CONCLUSION

In this study, electrochemical polymerization and characterization of polymers and copolymers of 3MT, 3OT and 3HT were made. The properties of the above monomers and their corresponding polymers and copolymers were also studied. This way of modification might be used as one method for production of various polymers for different applications.

Using polymer modified electrodes the detection of biological and environmental samples were examined. Studies on polymer or copolymer modified electrodes were made for use as an electroanalytical tool for detecting biological and environmental samples. Copolymers of 3MT and 3OT have shown a very good electrocatalytic activity towards the detection of ferricyanide, ascorbic acid, catechol and hydroquinone. The very interesting application observed was the simultaneous detection of two analytes in a given sample, which can avoid the disadvantages of the separation, operational complexity, time wastage and reagent consumption.

## REFERENCES


1. M. Depaoli, G. Casalbore, E.Girotto, and W. Gazotti, *Electrochimica Acta.*, **44** (1999) 2983.
2. a. Malinauskas, *Synth., Met.,* **107** (1999) 75.
   b. A. Kros, Stephan W. F. M. van Hövell, Nico A. J. M. Sommerdijk, and J. M. Nolte Roeland, *Adv. Mater.*, **20** (2001)1550.
3. M. Onoda, Y. Oshiyuki kato, H. Shonaka and K. Tada, *Electrical Engineering in Japan.*, **149** (2004) 120
4. P. Roy, M. Sudan, S. Takeyoshi, O.Gil, P. A. Fujishima, and T. Ohsakaa, *Electroanalysis.,* **16** (2004)1777
5. G. Yu and A. J. Heeger, *J. Appl. Phys*., **78** (1995) 4510.
6. P. Tuyen E. Nguyen U. Rammelt,W. Plieth, *J. Solid State Electrochem.,***7** (2003) 497
7. Teketel Yohannes, T. Solomon, and O. Inganas, *Synth. Met*., **82** (1996) 215.
8. Teketel Yohannes and O. Inganas, *Solar Materials and Solar Cells*, **51** (1998) 193.
9. Teketel Yohannes and O. Inganas, *Synth. Met.,***107** (1999) 97.
10. S. Lupu, C. Mihail, L. Pigani, R. Seeeber, N. Totir, and C. Zanardi, *Electrochemistry Communication.,* **4** (2004) 753.
11. G. Zotti, S. Zecchin, G. Schiavon, and L. Bert, *Micromol. Chem.Phys.,* **203** (2002) 1958.
12. B. Sean ,M. Ann Wilson, N. Dyer, Emmanuel and I. Antony G. *Microchem. Acta.,* **43** (2003)123.
13. P. Rajiv, R. C. Srivastava, P. C. Pandey, *J. Solid State Electrochem.*, **6** (2002) 203.
14. L. S. Roman, M. R. Andersson, Teketel Yohannes, and O. Inganas, *Adv. Mat.,* **9** (1997) 1164.
15. N. S. Sariciftci, *Prog . Quant. Electr.,* **19** (1995) 131.
16. Q. Pei and O. Inganas, *Polymer*, **34** (1993) 247.
17. M. Catellani, C. Arbizzani, M. Mastragostino, *Synth. Met.,* **69** (1995) 375.
18. S. Kuwabata, S. Ito, and H. Yoneyama, *J. Electrochem. Soc.,* **135** (1988) 1691.
19. Teketel Yohannes, J. C. Carlberg, O. Inganas, and T. Solomon, *Synth.Met.,* **88** (1997) 15.
20. S. Sadik, C. Chevrot, *Electrochemica Acta.,* **48** (2003) 733.
21. A. Gala*l, Electroanalysis,* **10** (1998**)** 121.

22. W. R. Salaneck, R.H. Friend and J. L. Bredas *Physics Reports,* **319** (1999) 231.
23. J. L. Bredas, R. R. Chance, and R. Silbey, *Phys. Rev. B*, **26** (1982) 5843.
24. J. L. Bredas, and G. B. Street, *Acc. Chem. Res*., **18** (1985) 319.
25. T. Yammato, and N. Hayashida, *Reactive and Functional Polymers*, **37** (1998) 17.
26. H. A.M. van Mullekoma, J. A.J.M. Vekemansb, E. E. Havingab, and E.W. Meijerb, *Materials Science and Engineering*, **32** (2001) 40.
27. M. A. Vorotyntsev and J. Heinze *Electrochimica Acta.,* **46** (2001) 3309.
28. P. Chandrasekhar, *Conducting Polymers Fundamentals and Applications: A Practical Approach,* Kluwer academic publisher,(2002).
29. G. Gustafsson, O. Inganas and J. O.Nilsson, , *Synth. Met.,* **26** (1988) 297.
30. Q. Pei and O. Inganas, *Synth. Met.,* **46** (1992) 353.
31. K. Tanaka, T. Shichiri, S. Wang and T. Yamabe, S*ynth. Met.,***24** (1988) 203.
32. D. Christian, M. Adam, P. Greg, K. Jansusz, and Z. Jin, *Synth. Met.*,**132** (2003) 197.
33. H. Neugebeauer, C. Kvarstorm, A. Crvavino, Teketel Yohannes, and N. S.Sariciftci, *Synth. Met.,* **116** (2001) 115.
34. W. j. Feast, J. Tsibouk, K.L. Pouwer, L. Groendaal, and E. W.Meijer, *Polymer,* **37** (1996) 5030.
35. R. L Elsenbaumer, K. Y. Jen, and R. Oboodi, *Synth. Met.,* **15** (1986) 169.
36. M. Sato, S. Tanaka, and K. Kaeriyama, *J. Chem. Soc. Chem. Commun*., (1986) 873.
37. S. Hardy, O. Chan, S. Choon , *Polym. Sci.,* **23** (1998) 1167.
38. G. J. Fleer, M. A. Cohen Stuart, J. M. H. M. Scheutjens, T, Cosgrov and B.Vincent, "*Polymers at Interfaces*", University Press,Cambridge (1993).
39. Q. pei, O. Inganas, J. Eric Osterholm and J. Laakso, *Polymer*, **34** (1993) 247.
40. G. Tourillon, and F. garnier, *J. of Electroanal.Chem*.,**161** (1984) 51.
41. M. A. Vorotyntsev and J. Heinze , *Electrochimica Acta,* **46** (2001) 3309.
42. K. Meerholz and J. Heinze, *Electrochim. Acta,* **41** (1996) 1854.
43. K. Meerholz and J. Heinze, *Angew*. *Chem.,* **29** (1990) 692.
44. S. W. Feldberg, *J. Am. Chem. Soc*., **106** (1984) 4671.
45. S. W. Feldberg and I. Rubinstein, *J. Electroanal*. *Chem*., **240** (1988) 1.
46. M. A. Vorotyntsev and J. P. Badiali, *Electrochim. Acta,* **39** (1994) 289.
47. M. Zagorska,. and B. Krische, *Polymer*, **31** (1990) 1379.

48. R. Cervini, X.C. Li, G. W. C. Spencer, A. B. Holmes, S. C. Moratti and R. H.Friend, *Synth. Met.,* **84** (1997) 359.
49. W. Kutner, J. Wang, M. Lher and R. P. Buck, *Pure & Appl. Chem.*, **70,** (1998) 1301.
50. Q. Honglani, and C. Zhang, *Electroanalysis,* **17** (2004) 120.
51. H. Zhao, Y. Z. Zhang, Z. and B.Yuanchin, *J.Anal.Lab.,***20** (2001) 70.
52. A. Malinauskas, *Synth. Met.,* **107** (1999) 75.
53. Z. Xu, X. Chen, Q. Xiaohu and S. Dong , *Electroanalysis,* **16** (2004) 684.
54. P. Rani Roy, M. Sudan Saha, T. Okajima and T. Ohsaka, *Electroanalysis,* **16** (2004) 289.
55. S. Lupu, A. Mucci, L. Pigani, R. Seeber, and C. Zanardib, *Electroanalysis,* **14** (2002) 519.
56. S. ztemiz, G. Beaucage, O. Ceylan and H. B. Mark, *J. solid state electrochemistry,* **8** (2004) 928.
57. J. P. Skabara, D. M. Roberts, I. M. Serebryakov and C. Pozo-Gonzalo, *Chem. Commun.*, (2000) 1005.
58. H. Sheng Wang, D. Qian Huang, and R. Min Liu, *J. Electroanalytical Chem., **570*** (2004) 83.
59. J. Wang, *Analytical Electrochemistry*, Wiley-VCH, New York, 1994, p.164.
60. M. B.Smith and j. March, *Advanced Organic Chemistry, Reactions, Mechanisms and Structure, 5th Edition,* John wiley and Sons, INC, NewYork, 2001, p.1511.
61. J. M. Zen and P. J. Chen, *Electroanalysis,* **10** (1998) 12.